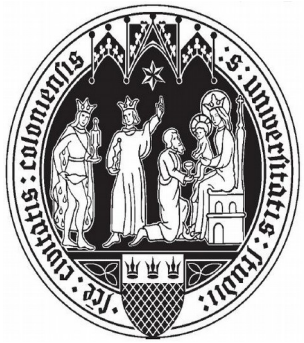

[CII] Optical Depth and Self-Absorption in Galactic Sources

Cristian Guevara

I. Physikalisches Institut – Universität zu Köln

With Jürgen Stuzki, Volker Ossenkopf-Okada, Robert Simon, Juan Pablo Pérez-Beaupuits, Henrik Beuther, Simon Bihr, Ronan Higgins, Urs Graf and Rolf Güsten

Outline

- Motivation
- [^{13}CII] hyper-fine structure line
- Description of the Sources
- Zeroth Order Analysis: [^{12}CII] Optical Depth and Abundance Ratio
- Multi-component Analysis: Double Layer Model
- [^{12}CII]/[^{13}CII] Abundance Ratio
- [NII] Observations
- Origin of the Gas
- Summary
- Future Work

Cristian Guevara,
Ph1, Uni zu Köln

Motivation

- **First detection of the [CII] fine-structure emission line (Russell et. al. 1980):**

"Optical depth effects in the 157 μm line may be significant but have not been take into account in our calculation because our data is still too restricted"

Cristian Guevara,
Ph1, Uni zu Köln

[^{13}CII] hyper-fine structure line

- **C^+ has only two fine structure levels in the ground state with an energy difference of 91.25 K. The ionization potential of carbon is 11.2 eV.**
- **Emission is produced by collisional excitation followed by radiative decay at 1.9 THz.**
- **The hyper-fine structure of the $^{13}C^+$ isotope due to the extra neutron, it is splitted into three hfs-components.**

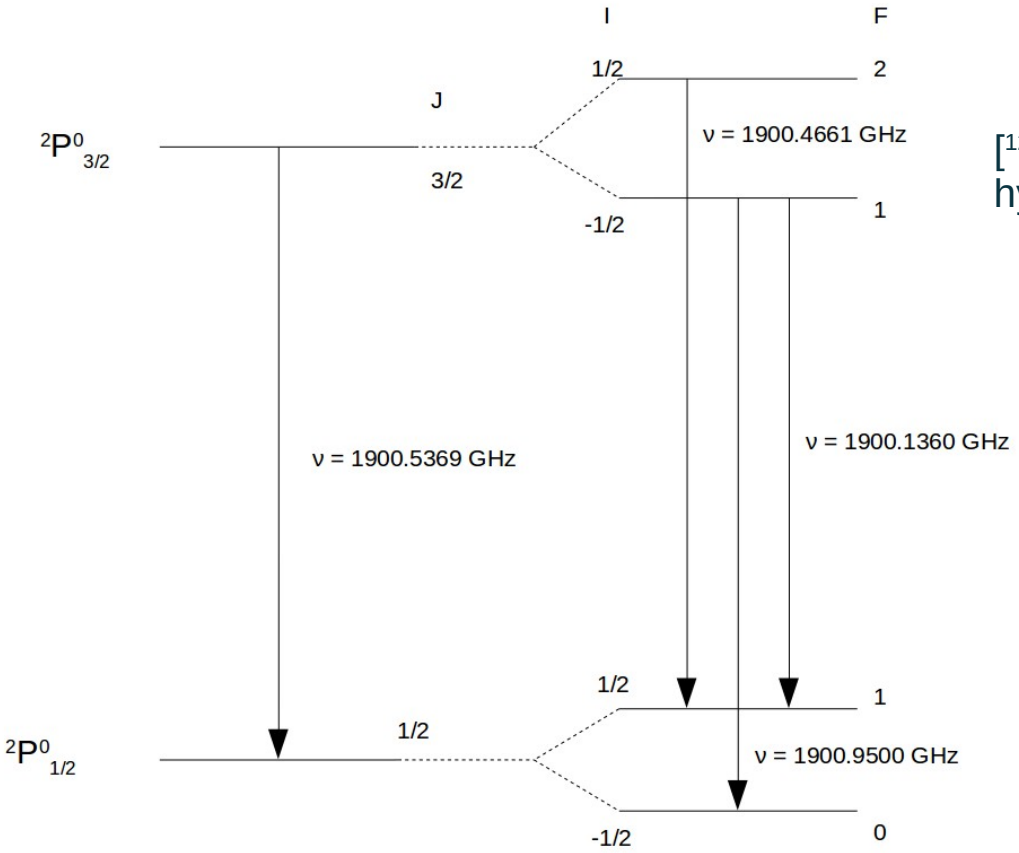

[^{12}CII] fine structure and [^{13}CII] hyper-fine structure levels

Cristian Guevara,
Ph1, Uni zu Köln

[^{13}CII] hyper-fine structure line

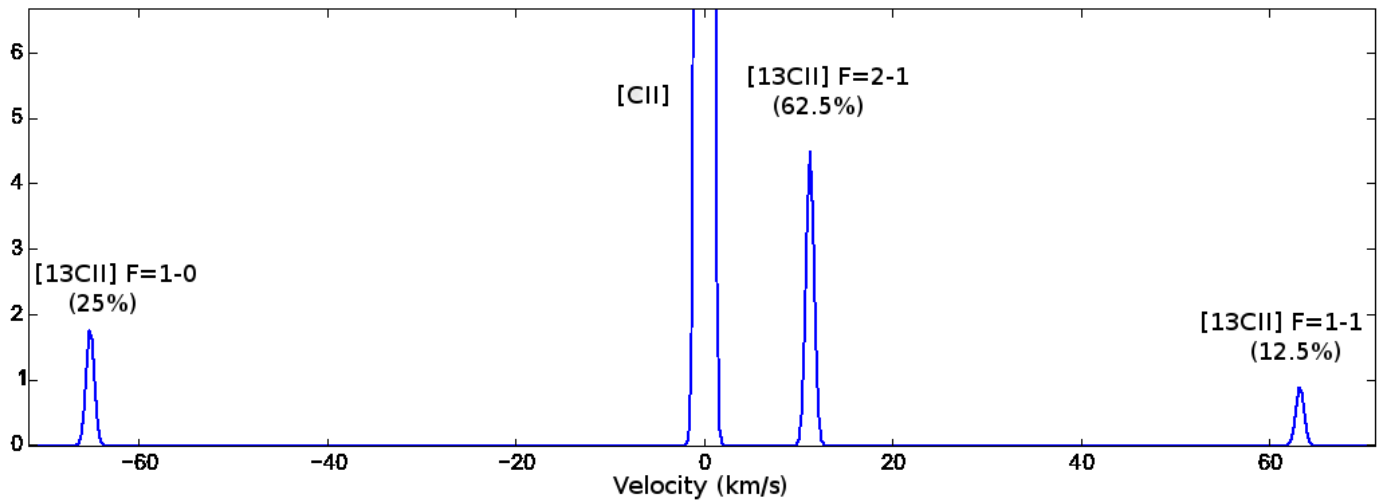

[^{12}CII] and [^{13}CII] spectral signature

Line	Statistical g_u	Weight g_l	Frequency ν (GHz)	Vel. offset $\delta v_{F\rightarrow F'}$ (km/s)	Relative intensity $s_{F\rightarrow F'}$
[^{12}CII] $^2P_{3/2}-^2P_{1/2}$	4	2	1900.5369	0	–
[^{13}CII] F=2→1	5	3	1900.4661	+11.2	0.625
[^{13}CII] F=1→0	3	1	1900.9500	-65.2	0.250
[^{13}CII] F=1→1	3	3	1900.1360	+63.2	0.125

Cristian Guevara,
Ph1, Uni zu Köln

Description of the Sources

M43

- **M43 is a close-by ideal spherical nebula with a single exciting star in the center, an early B type star.**
- **It is located northeast of the Orion nebula with a distance of 389 pc.**
- **Due to its close distance, its simple spherical geometry and a single ionization source, M43 is well suited as a simple, properly characterized test case.**

M43 Visible + IR composite image

Credit: ESA/Hubble NASA

Cristian Guevara,
Ph1, Uni zu Köln

Description of the Sources

Horsehead PDR

- **Horsehead PDR is a dark cloud filament protruding out of the Orion Molecular Complex.**
- **The region is located at a distance of 360 pc.**
- **It has an edge-on geometry illuminated by two OB systems with a moderate far-UV intensity of 100.**

Horsehead IR image

Credit: ESO

Description of the Sources

Monoceros R2

- **Monoceros R2 (MonR2) is an ultra compact HII region located at 830 pc.**
- **The region contains a reflection nebula and the UCHII is surrounded by several PDRs.**
- **IRS1 is the main ionization source with high UV field > 10^5.**

Monoceros R2 IR image

Credit: VISTA/ESO

Description of the Sources

M17

- **It is considered one of the brightest and most massive star forming regions in the Galaxy, located at 1.9 kpc of distance.**
- **The cloud is illuminated by a cluster (>100) of OB stars.**
- **M17SW presents an edge-on geometry, very well suited for studying the PDR structure.**

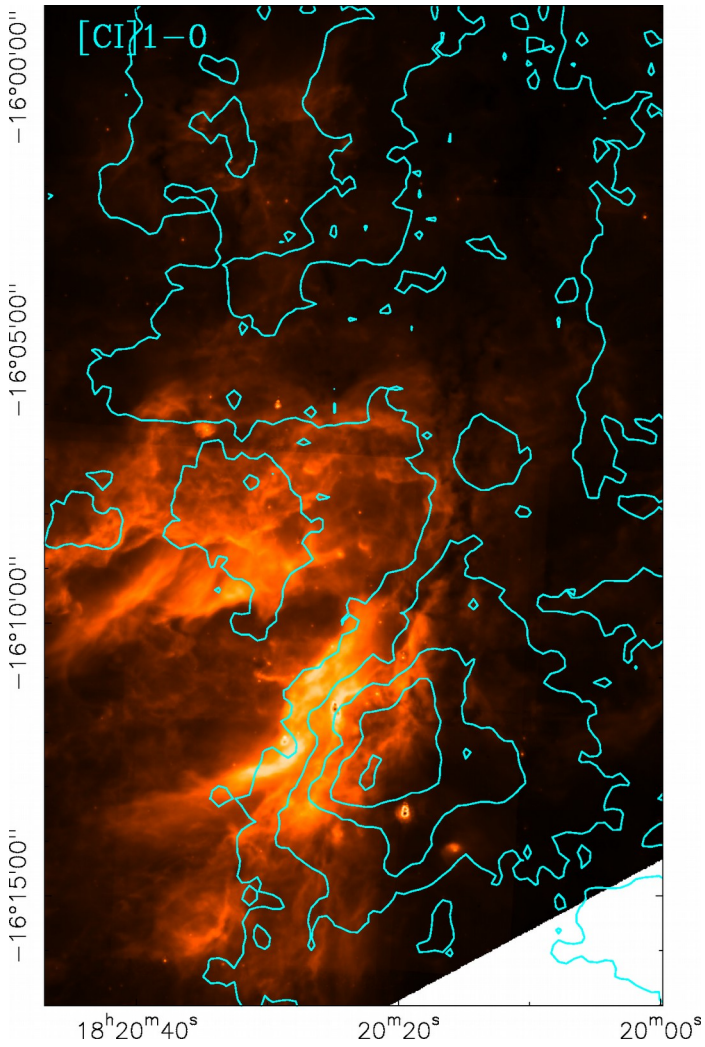

M17 8 μm Spitzer map and [CI] $^3P_1$-$^3P_0$ NANTEN2/SMART integrated intensity map in contours

Cristian Guevara,
Ph1, Uni zu Köln

Observations

- **Observations were done using the SOFIA/upGREAT 7x2 pixels array receiver between 2015 and 2017.**
- **The array was centered around the [CII] peak.**
- **Deep integration (30-80 min) with high S/N ~ 300 for [^{12}CII] and ~ 7 for [^{13}CII] F=1-0 with a rms of 0.1-0.3 K.**

M17SW [CII] integrated intensity map (Pérez-Beaupuits et al. 2012) with the 7 upGREAT pixels

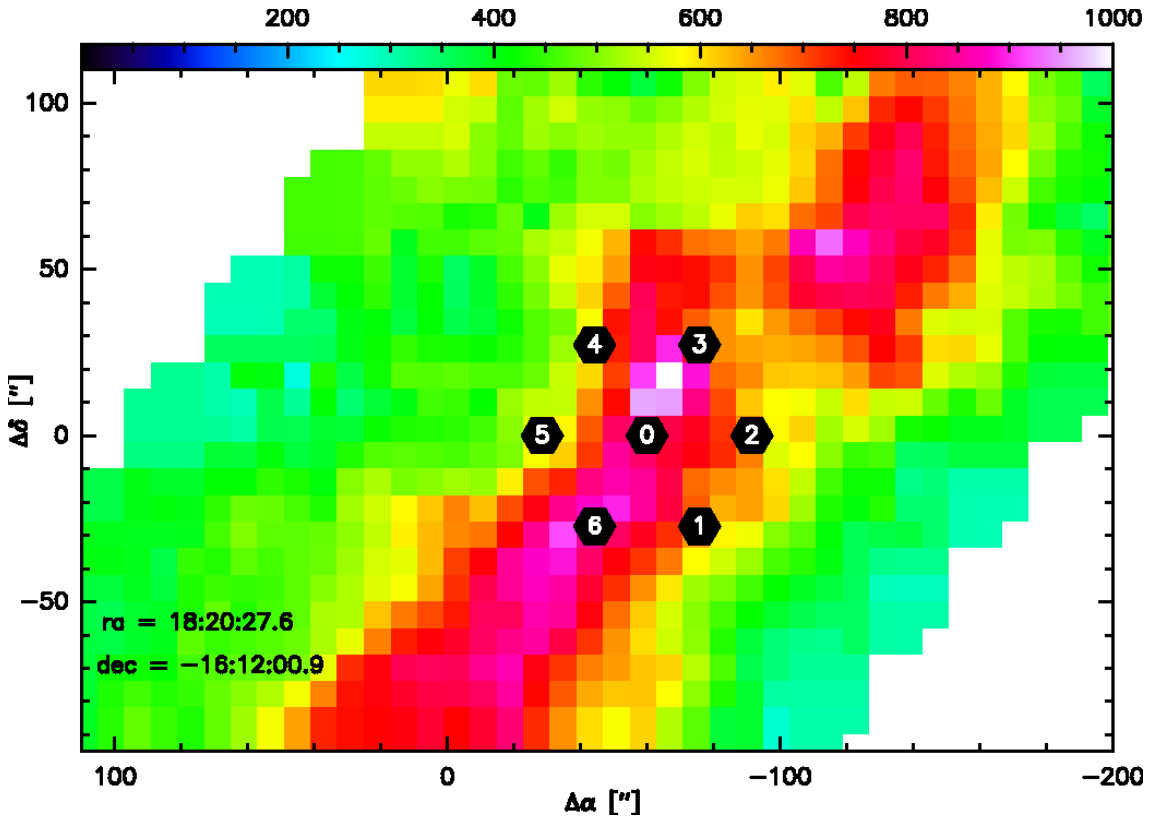

Cristian Guevara,
Ph1, Uni zu Köln

Observations

- **Observations were done using the SOFIA/upGREAT 7x2 pixels array receiver between 2015 and 2017.**
- **The array was centered around the [CII] peak.**
- **Deep integration (30-80 min) with high S/N ~ 300 for [^{12}CII] and ~ 7 for [^{13}CII] F=1-0 with a rms of 0.1-0.3 K.**

Horsehead PDR [CII] integrated intensity map with the 7 upGREAT pixels

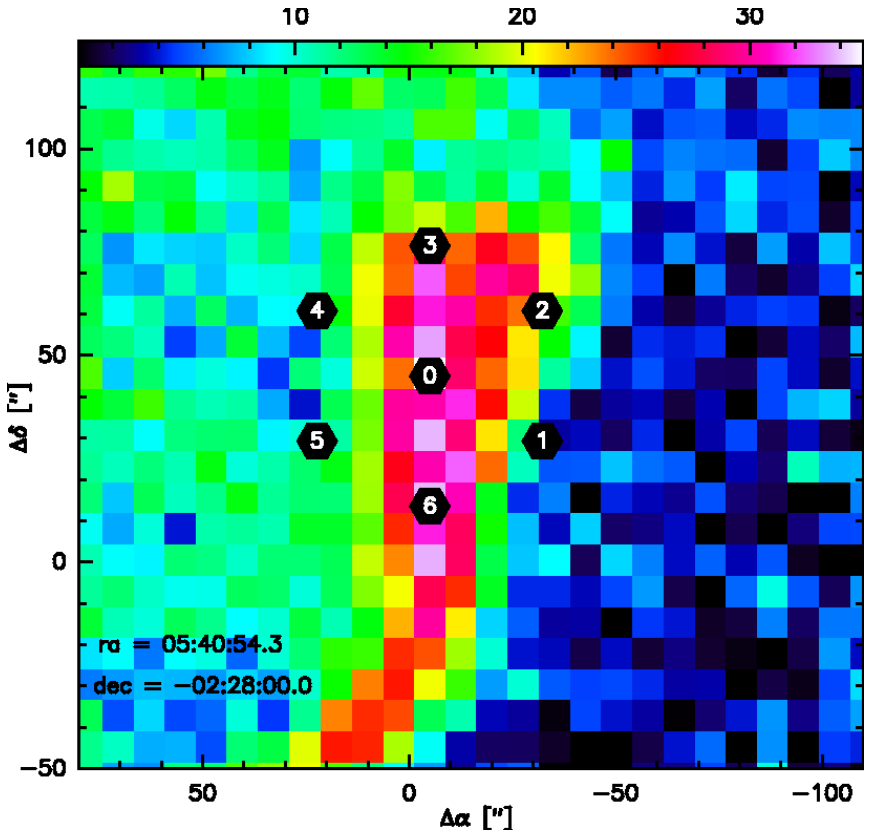

Zeroth Order Analysis

- **As a first approximation, it was assumed that the source has a single homogeneous layer with the same excitation temperature (T_{ex}) for both isotopes.**
- **[^{13}CII] was scaled up assuming the elemental abundance ratio $^{12}C/^{13}C$ for the different sources.**

M17SW [CII] observations

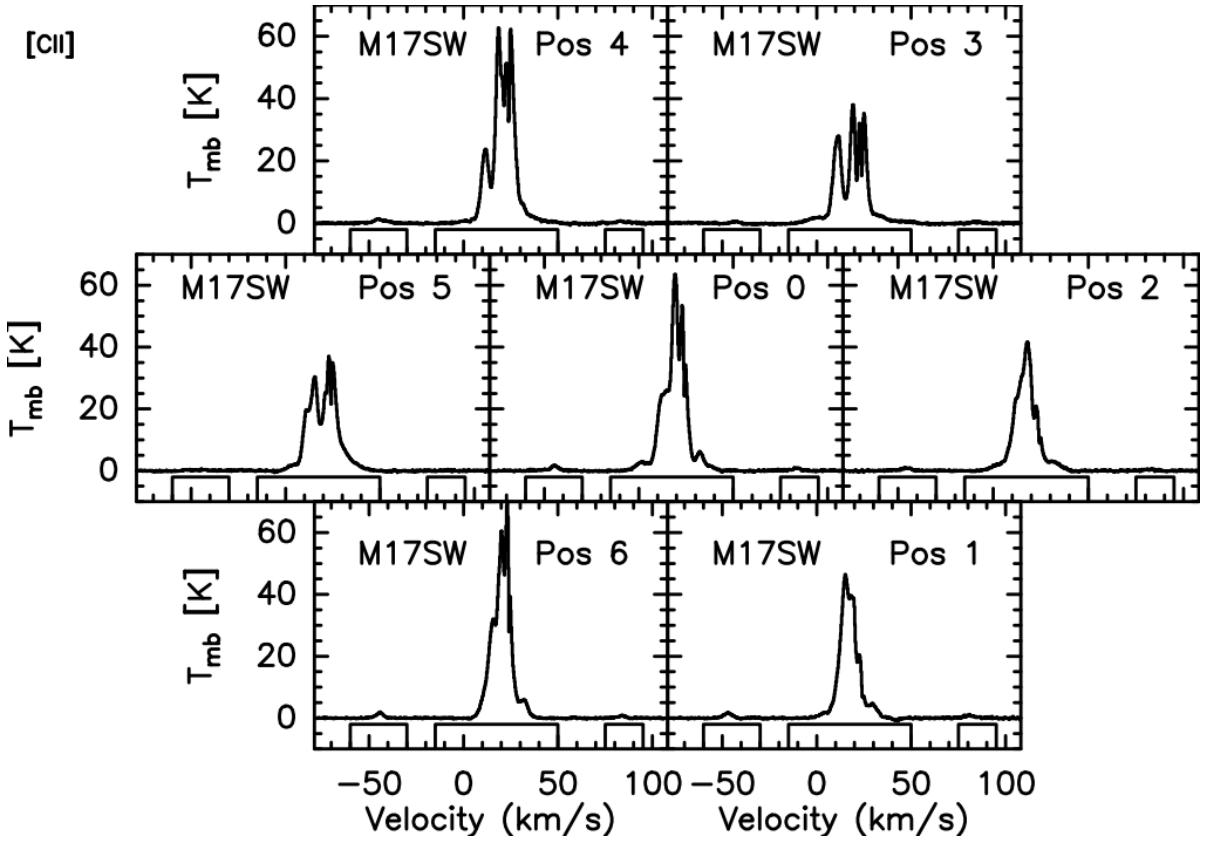

Cristian Guevara,
Ph1, Uni zu Köln

Zeroth Order Analysis

- **[^{13}CII] overshoots the [^{12}CII] emission at the line center and matches at the line wings for M43 and Horsehead PDR.**

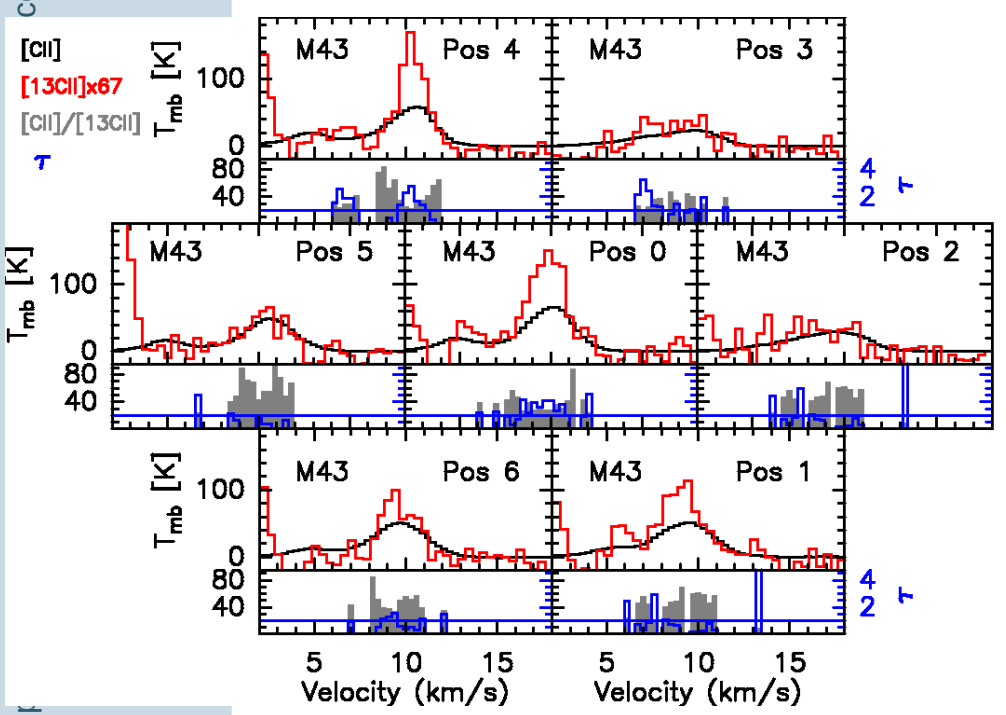

M43 comparison between [^{12}CII] and the scaled up [^{13}CII]

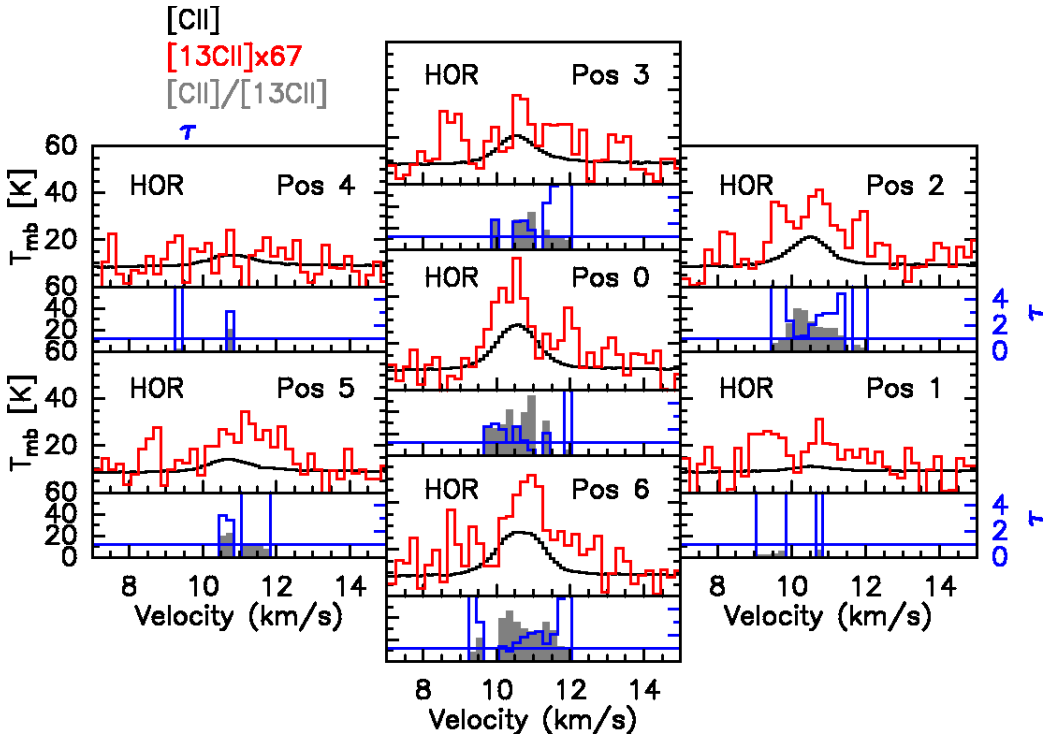

HOR PDR comparison between [^{12}CII] and the scaled up [^{13}CII]

Zeroth Order Analysis

- **The [CII] optical depth was estimated from the [^{12}CII] and [^{13}CII] line.**

$$\frac{T_{mb,12}(v)}{T_{mb,13,tot}(v)} \simeq \frac{1 - e^{-\tau(v_{12})}\,\alpha^{+}}{\tau(v_{12})}$$

- **The emission is optically thick in the line center with a τ between 1 and 2 for M42 and HOR PDR.**

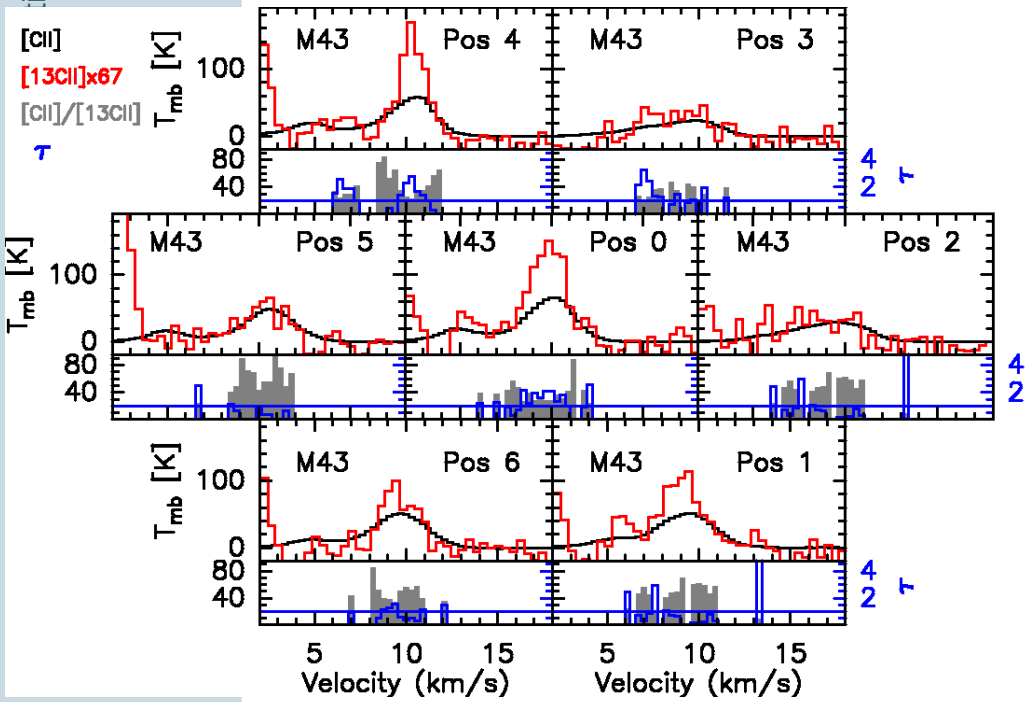

M43 comparison between [^{12}CII] and the scaled up [^{13}CII]

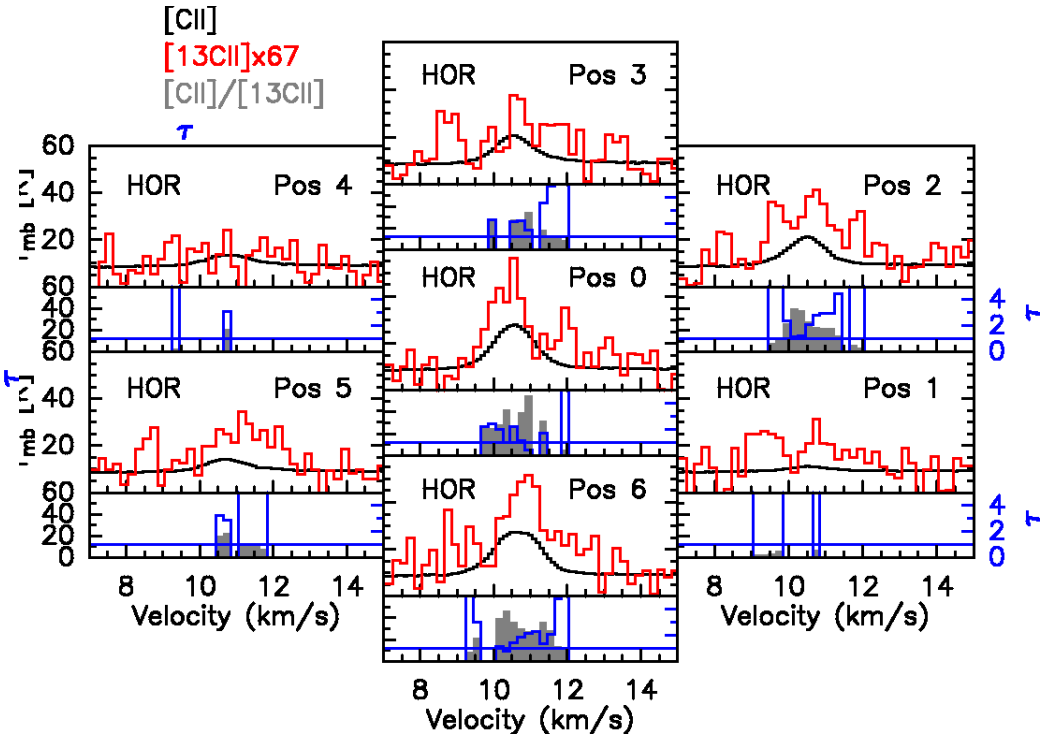

HOR PDR comparison between [^{12}CII] and the scaled up [^{13}CII]

Zeroth Order Analysis

- **[^{13}CII] overshoots the [^{12}CII] emission at the line center and matches at the line wings for MonR2 and M17SW.**
- **[^{12}CII] line profiles shows absorption dips not present in [^{13}CII] for MonR2 and M17SW.**

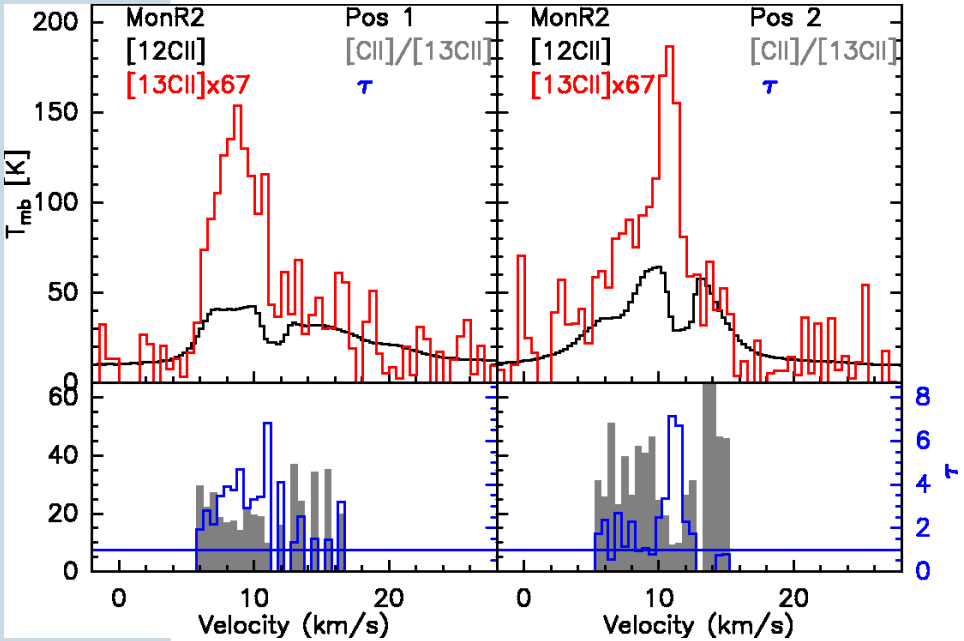

MONR2 comparison between [^{12}CII] and the scaled up [^{13}CII]

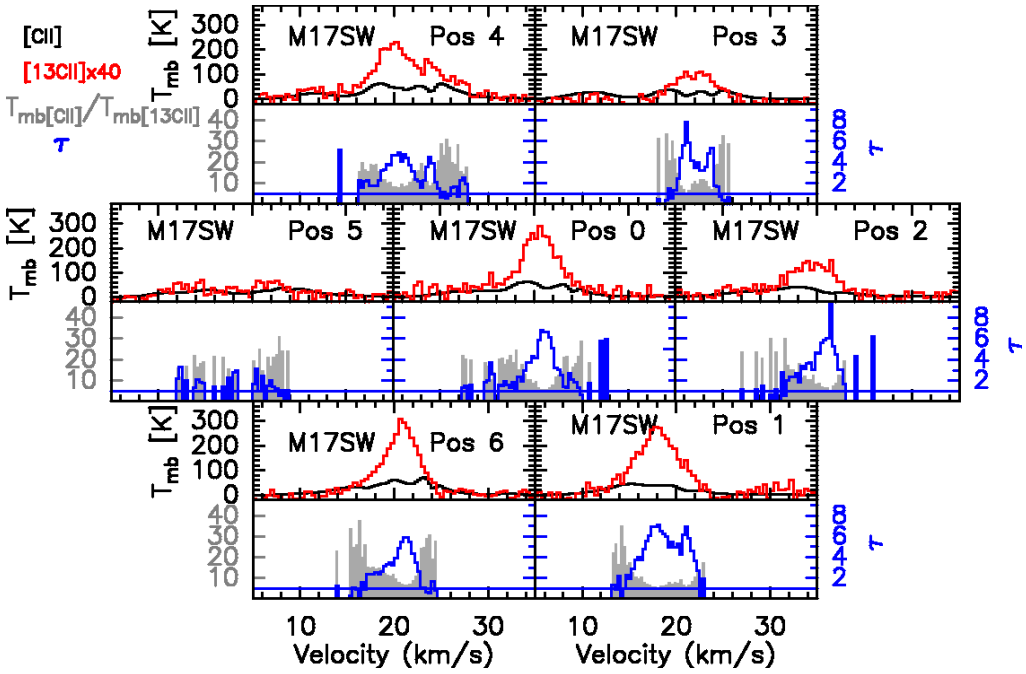

M17SW comparison between [^{12}CII] and the scaled up [^{13}CII]

Cristian Guevara,
Ph1, Uni zu Köln

Zeroth Order Analysis

- **The [CII] optical depth was estimated from the [^{12}CII] and [^{13}CII] line.**

$$\frac{T_{mb,12}(v)}{T_{mb,13,tot}(v)} \simeq \frac{1 - e^{-\tau(v_{12})}\,\alpha^{+}}{\tau(v_{12})}$$

- **The emission is optically thick in the line center with a τ between 4 and 8 for MONR2 and M17SW**

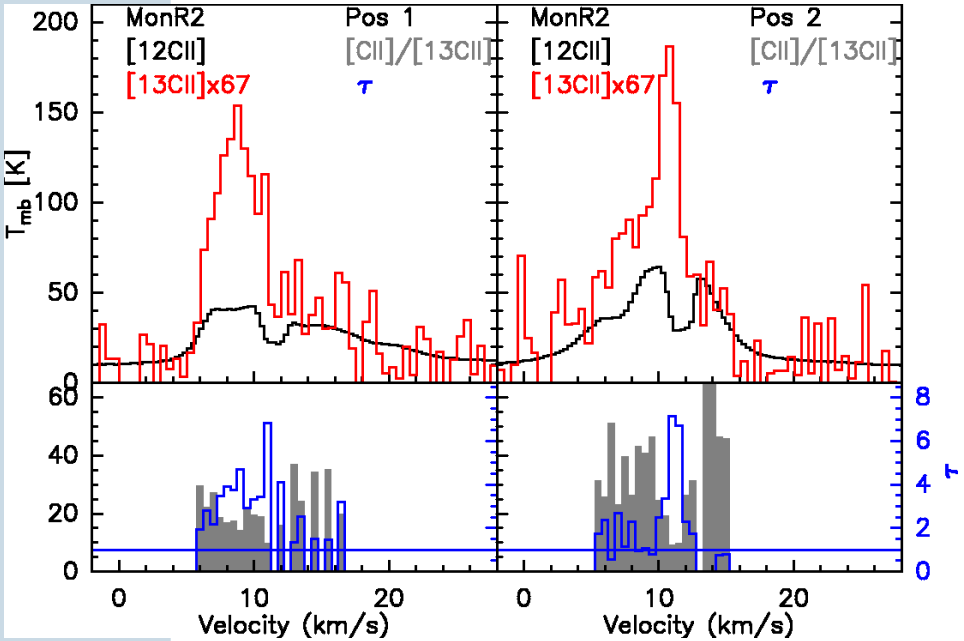

MONR2 comparison between [^{12}CII] and the scaled up [^{13}CII]

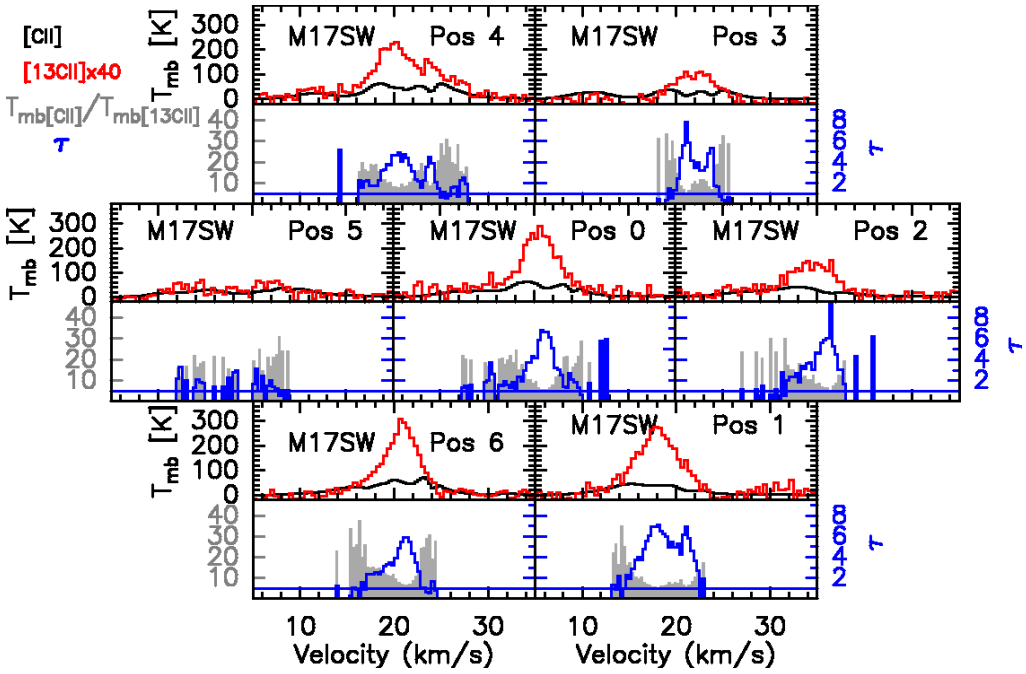

M17SW comparison between [^{12}CII] and the scaled up [^{13}CII]

Cristian Guevara,
Ph1, Uni zu Köln

Zeroth Order Analysis

- **We also estimated the column density directly from the integrated intensity for [12CII] and the scaled-up [13CII] by the elemental abundance ratio.**

Positions	[^{13}CII]				Optically thin [^{12}CII]			Ratio
	[^{13}CII] Int. Intensity (K km/s)	N_{min}([^{13}CII]) (cm^{-2})	N_{min}([CII])[a] [^{13}CII] (cm^{-2})	$A_{v,min}$[b] [^{13}CII] (mag.)	[^{12}CII] Int. Intensity (K km/s)	N_{min}([CII])[c] [^{12}CII] (cm^{-2})	$A_{v,min}$[d] [^{12}CII] (mag.)	$\frac{A_{v,min}([^{13}CII])^{b}}{A_{v,min}([^{12}CII])^{d}}$
M43 0	5.5	2.5E16	1.7E18	7.4	283.1	1.3E18	5.6	1.3
M43 1	4.3	1.9E16	1.3E18	5.7	249.2	1.1E18	4.9	1.2
M43 2	2.6	1.2E16	7.7E17	3.4	172.2	7.7E17	3.4	1.0
M43 3	2.6	1.1E16	7.6E17	3.4	134.0	6.0E17	2.6	1.3
M43 4	5.5	2.5E16	1.7E18	7.4	270.1	1.2E18	5.3	1.4
M43 5	3.7	1.6E16	1.1E18	4.9	227.4	1.0E18	4.5	1.1
M43 6	4.1	1.8E16	1.2E18	5.4	237.9	1.1E18	4.7	1.1
HOR 0	1.2	5.3E15	3.6E17	1.6	39.6	1.8E17	0.8	2.0
HOR 1	0.7	3.1E15	2.1E17	0.9	11.2	5.0E16	0.2	4.2
HOR 2	1.4	6.1E15	4.1E17	1.8	26.6	1.2E17	0.5	3.4
HOR 3	1.0	4.7E15	3.1E17	1.4	25.7	1.1E17	0.5	2.7
HOR 4	0.3	1.2E15	8.4E17	0.4	14.8	6.6E16	0.3	1.3
HOR 5	0.9	3.9E15	2.6E17	1.2	14.7	6.5E16	0.3	4.0
HOR 6	1.6	7.0E15	4.7E17	2.1	41.5	1.9E17	0.8	2.5
MonR2 1	12.2	5.5E16	3.7E18	16.3	410.8	1.8E18	8.1	2.0
MonR2 2	11.4	5.1E16	3.4E18	15.2	477.0	2.1E18	9.5	1.6
M17SW 0	41.6	1.9E17	7.4E18	33.0	657.2	2.9E18	13.1	2.5
M17SW 1	39.1	1.7E17	7.0E18	31.1	460.1	2.1E18	9.1	3.4
M17SW 2	26.9	1.2E17	4.8E18	21.3	458.1	2.0E18	9.1	2.3
M17SW 3	16.5	7.4E16	2.9E18	13.1	489.9	2.2E18	9.7	1.3
M17SW 4	45.1	2.0E17	8.1E18	35.9	722.7	3.2E18	14.4	2.5
M17SW 5	14.1	6.3E16	2.5E18	11.2	521.7	2.3E18	10.4	1.1
M17SW 6	34.3	1.5E17	6.1E18	27.3	617.7	2.8E18	12.3	2.2

[a] [^{12}CII] column density derived from the scaled-up [^{13}CII] column density.
[b] [^{12}CII] equivalent visual extinction derived from the scaled-up [^{13}CII] column density.
[c] [^{12}CII] column density derived directly from the [^{12}CII] integrated intensity assuming optically thin regime.
[d] [^{12}CII] equivalent visual extinction derived directly from the [^{12}CII] integrated intensity assuming optically thin regime.

Cristian Guevara,
Ph1, Uni zu Köln

Multi-component Analysis

- The [^{12}CII] spectra with complex velocity structure and absorption dips shows that the single layer assumption is insufficient.
- The objective is to explain the [^{12}CII] and [^{13}CII] line profile by a composition of multiple Gaussians components.
- The model contains 2 layers, a background emission layer and a foreground absorption layer.

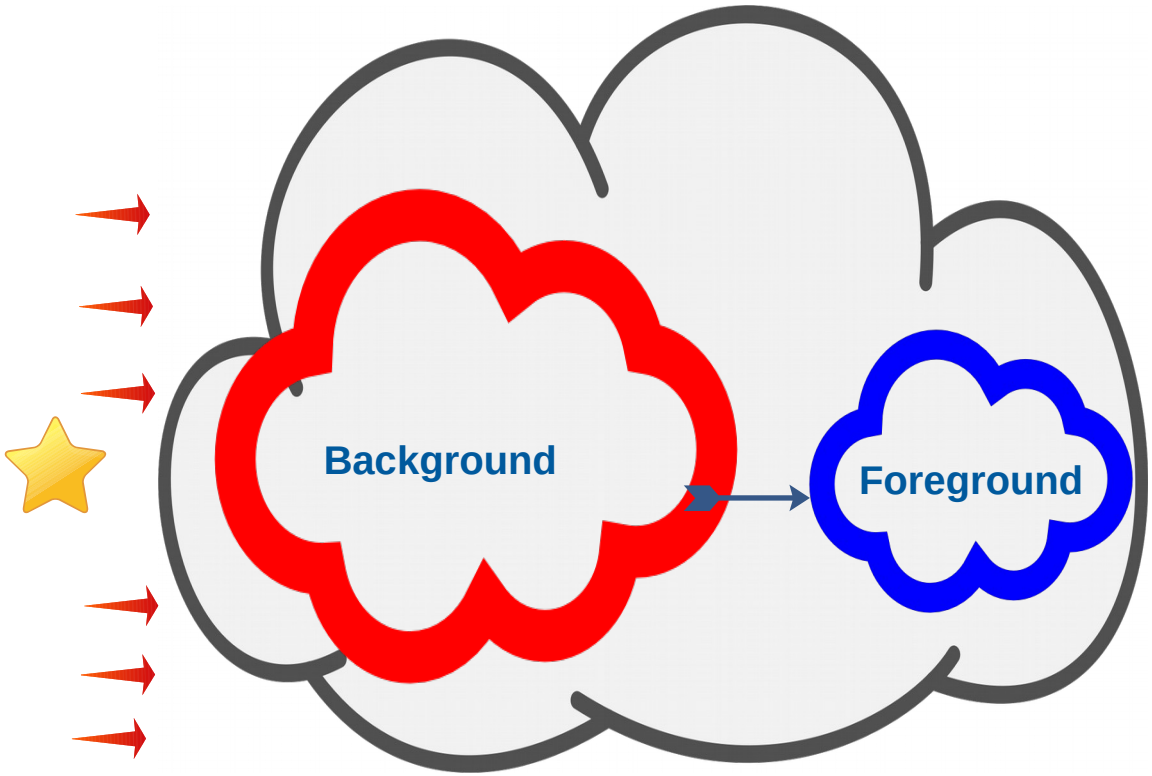

Credit: getdrawings.com, pngtree.com, iconsplace.com

Credit: NASA/Jim Ross

Cristian Guevara,
Ph1, Uni zu Köln

Multi-component Analysis

- **The plan is to use the radiative transfer equation to derive:**

- The excitation temperature (T_{ex})

- [^{12}CII] column density (N_{12}(CII))

- The velocity center (v_{LSR})

- The FWHM velocity width (Δv_{LSR}).

$$\tau_i(v) = \Phi_i(v) \frac{g_u}{g_l} \frac{c^3}{8\pi\nu^3} A_{ul} N_{12,i}(CII) \frac{\left(1 - e^{-T_0/T_{ex,i}}\right)}{1 + \frac{g_u}{g_l} e^{-T_0/T_{ex,i}}}$$

$$T_{mb}(v) = \left[\sum_{i_b} \mathcal{J}_\nu(T_{ex,i_b}) \left(1 - e^{-\tau_{i_b}(v)}\right) \right] e^{-\sum_{i_f} \tau_{i_f}(v)} + \sum_{i_f} \mathcal{J}_\nu(T_{ex,i_f}) \left(1 - e^{-\tau_{i_f}(v)}\right)$$

Cristian Guevara,
Ph1, Uni zu Köln

Multi-component Analysis

- **Three basic assumptions were done:**
  - **T_{ex} is the same for [^{12}CII] and [^{13}CII].**
  - **[^{13}CII] is optically thin.**
  - **If [^{12}CII] does not have a visible [^{13}CII] counterpart above noise level, [^{12}CII] emission is not affected by self-absorption effects.**

Multi-component Analysis

- **Fitting process: 1st the [13CII] emission is fitted, fixing T_{ex}.**

Model
Data
Background
Foreground τ

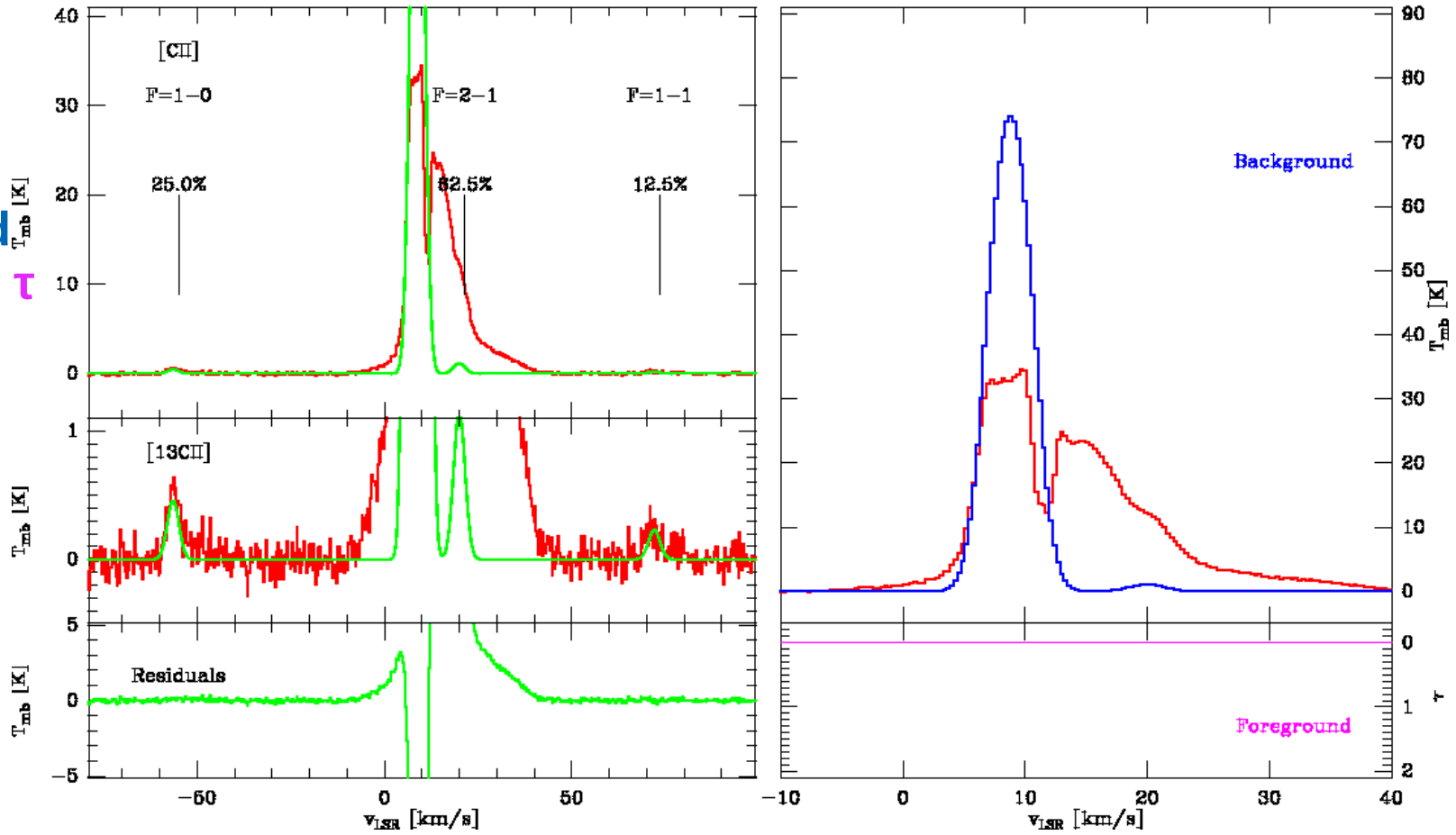

MONR2 position 1

Multi-component Analysis

- **Fitting process: 2nd the remaining [^{12}CII] emission is fitted, fixing T_{ex}.**

Model
Data
Background
Foreground τ

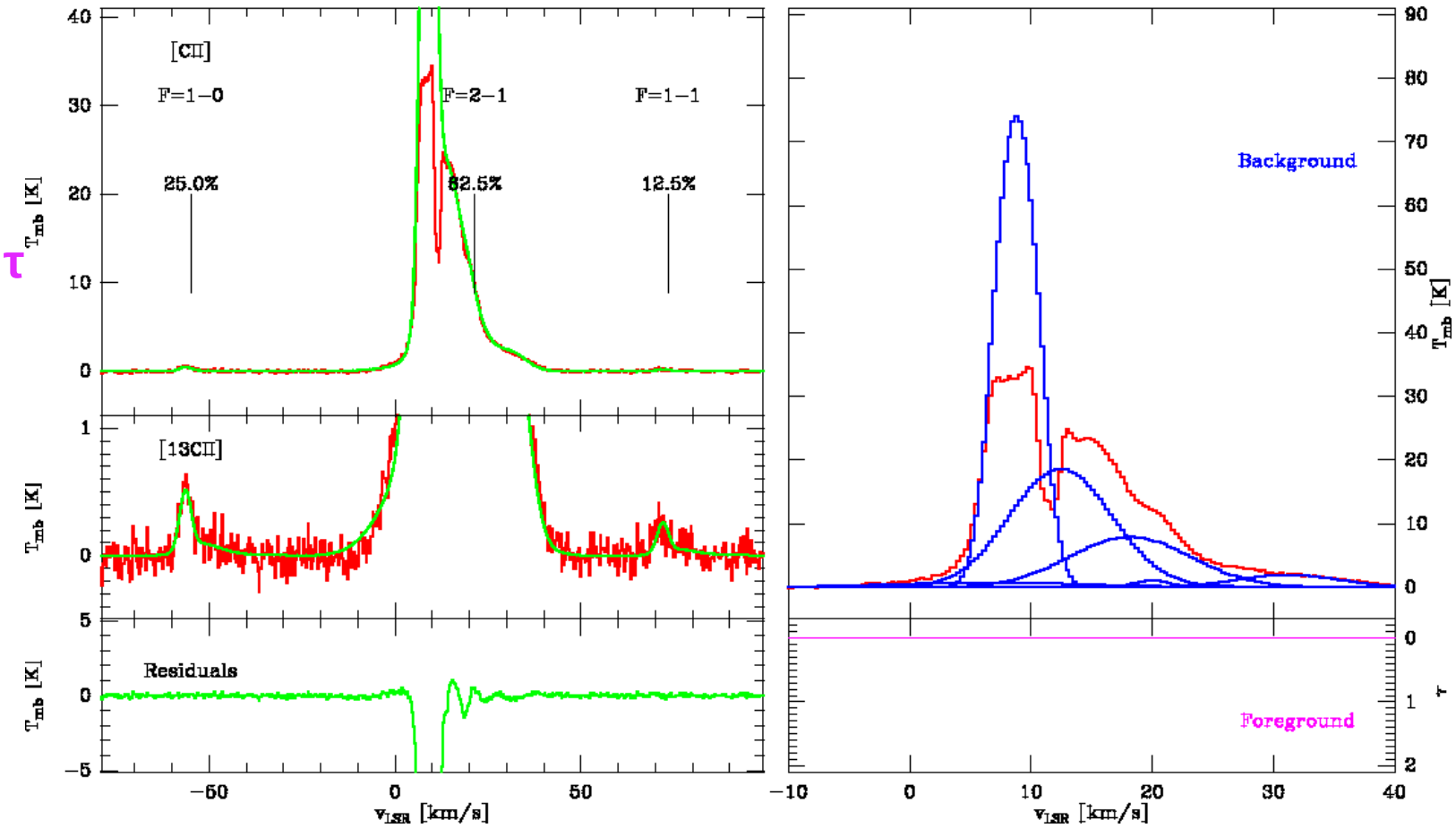

MONR2 position 1

Multi-component Analysis

- **Fitting process: 3rd as the fitted line profile overshoots the observed one, the foreground absorption features are fitted with a fixed lower T_{ex}.**

Model
Data
Background
Foreground τ

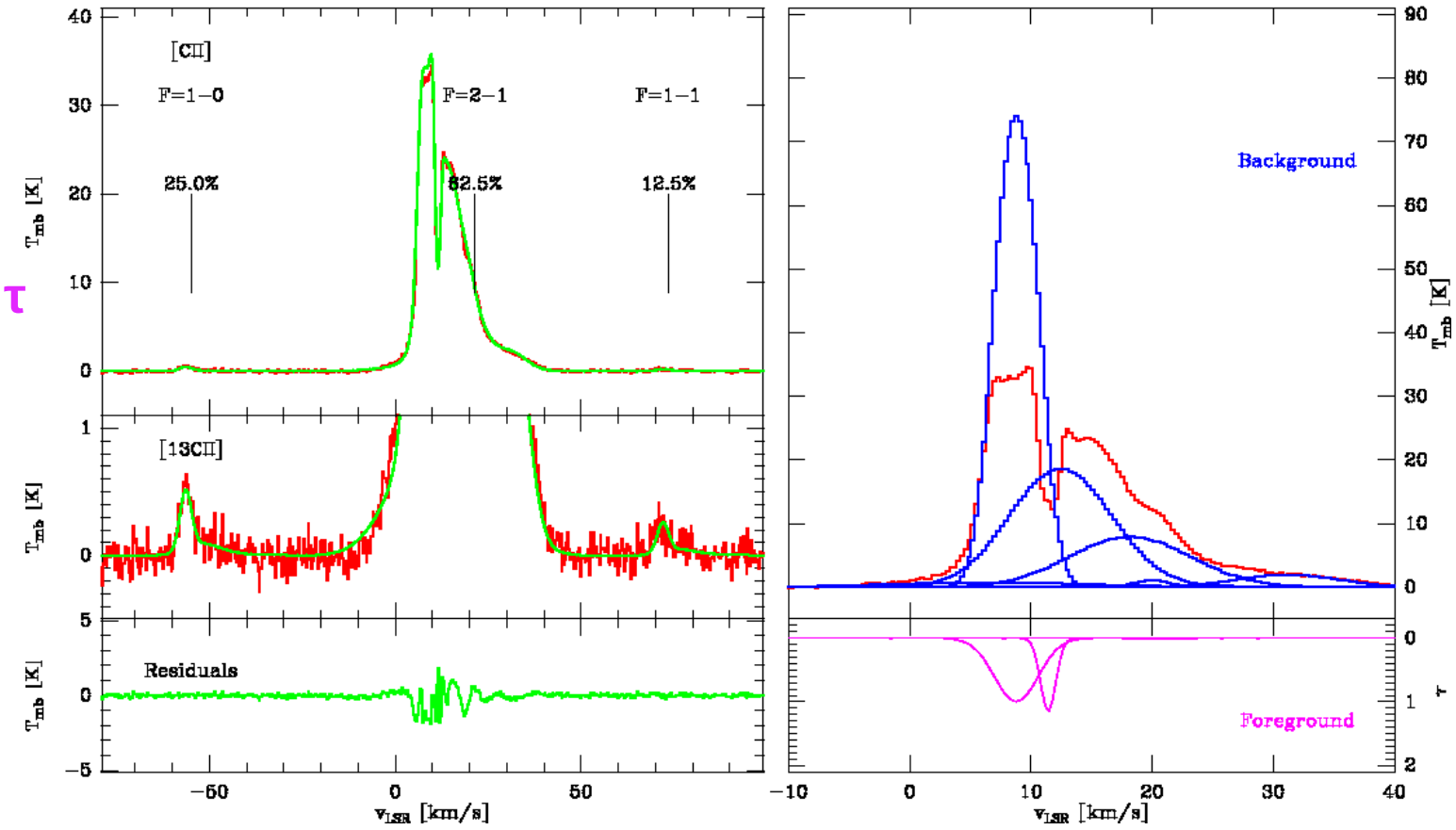

MONR2 position 1

Multi-component Analysis

- **For M43 and Horsehead PDR, due to the absence of absorption features, the background temperature was fitted, with a T_{ex} of 100 K (M43) and 30 K (HOR).**

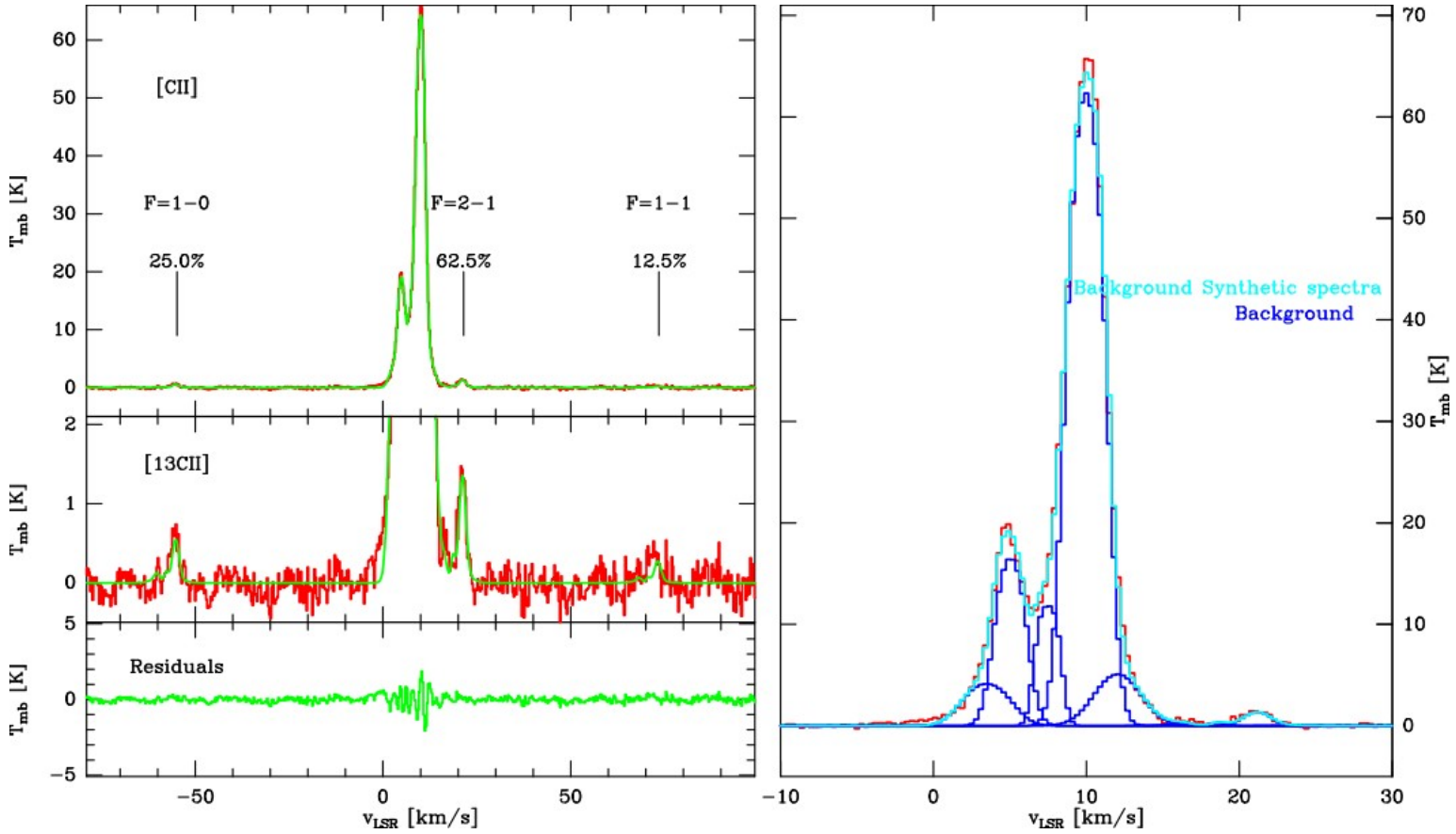

M43 position 0

Multi-component Analysis

- **The total [^{12}CII] column density for the different positions varied between 1x10^{18} and 4x10^{18} cm^{-2} for M43 and 3.6x10^{17} and 1.3x10^{18} cm^{-2} for HOR, with an Av between 4.9 and 18.3 mag for M43 and 1.6 to 5.8 mag for HOR.**

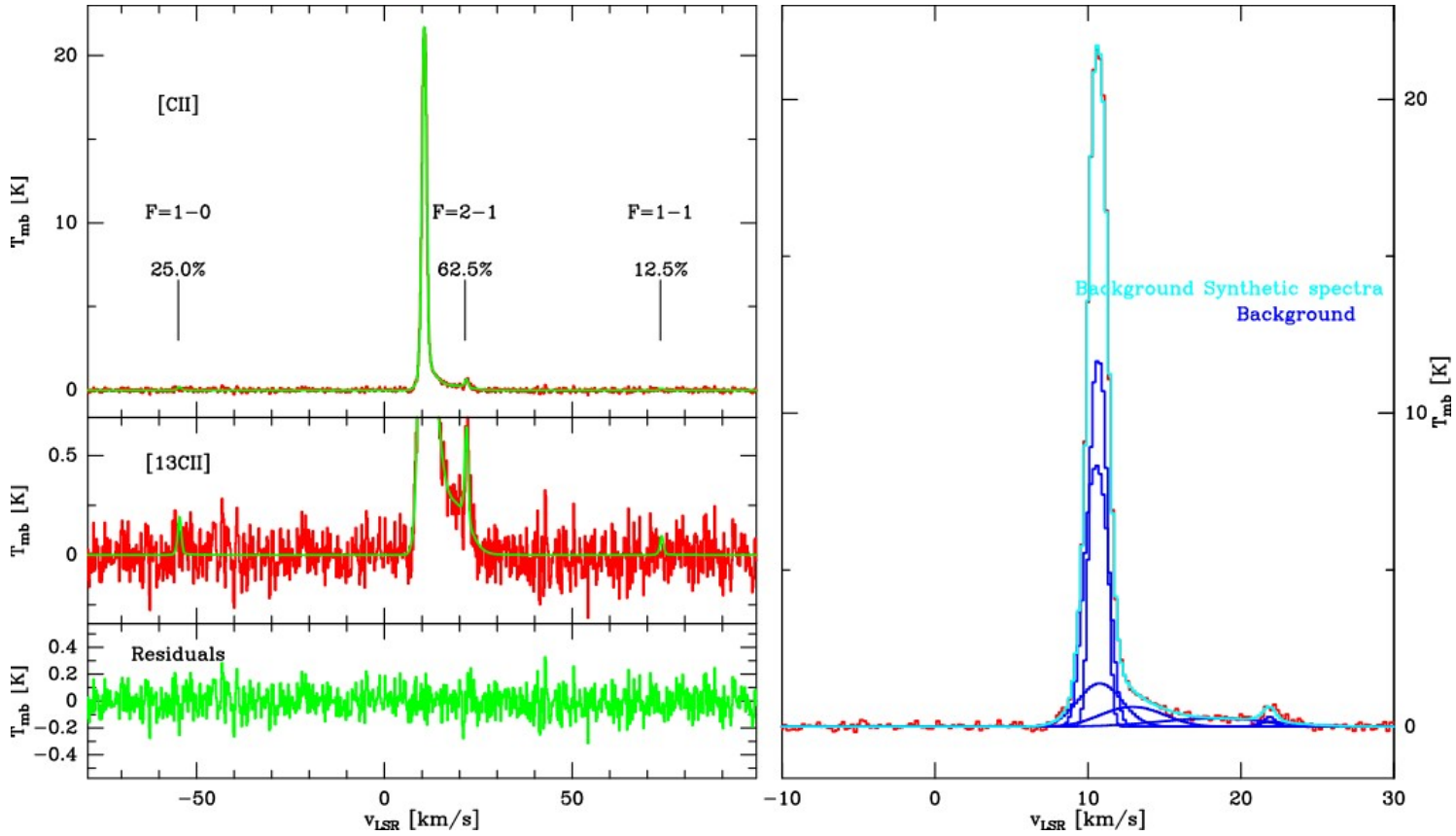

HOR PDR position 6

Multi-component Analysis

- For MONR2 and M17SW, sources that present absorption dips:
- The background is composed by high temperature broad emission components with extremely high column density.
- The foreground is composed by low temperature narrow absorption notches with high column density.

Model
Data
Background
Foreground τ

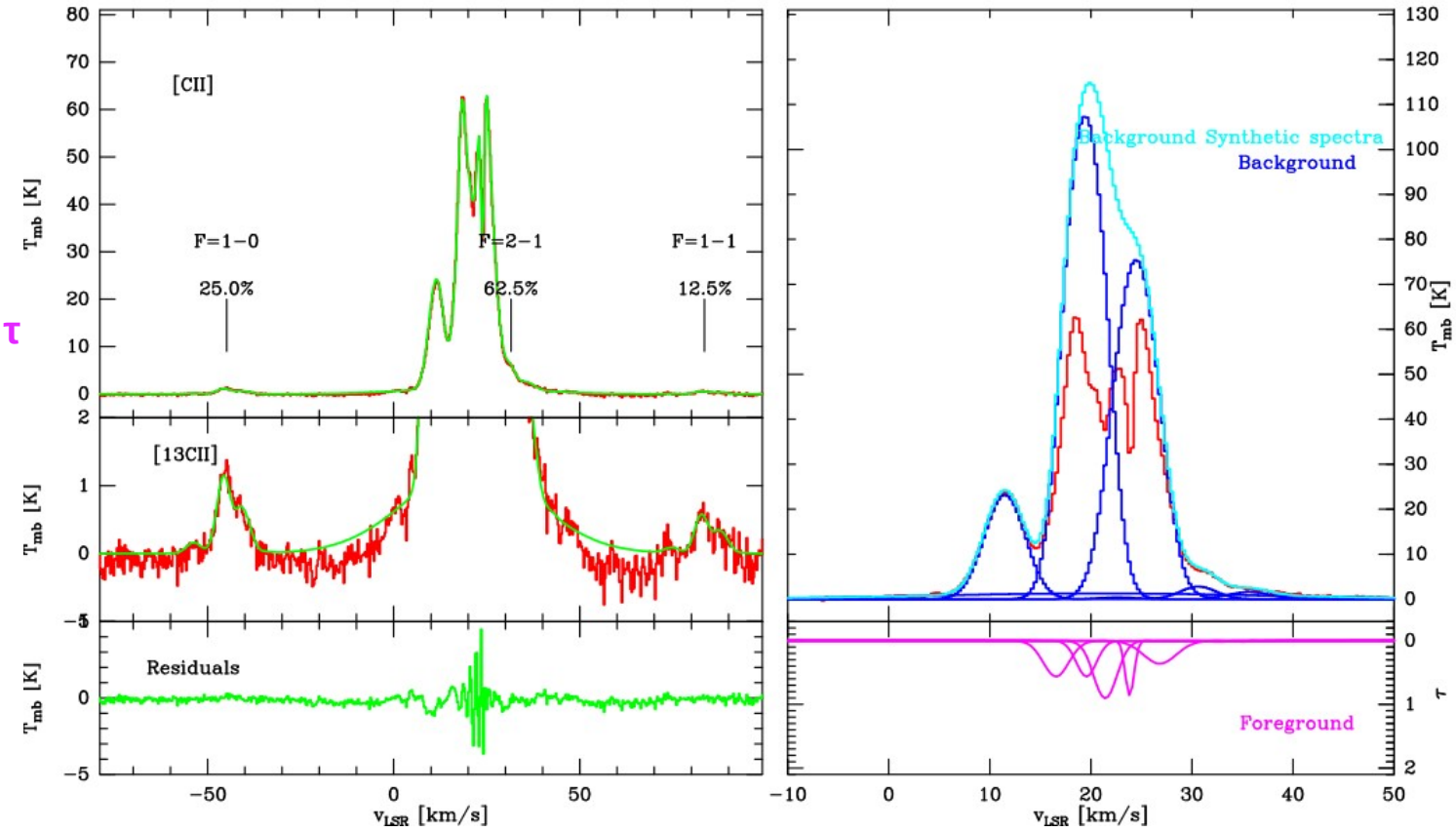

M17SW position 4

Multi-component Analysis

- **MONR2 fitted parameters**

	Background	Foreground
Excitation	150 K	20 K
Column Density	$4.2 \times 10^{18} - 4.7 \times 10^{18}$	$8.3 \times 10^{17} - 6.4 \times 10^{18}$
Equivalent visual extinction (Av)	19 - 21 mag	3.7 – 2.9 mag

Model
Data
Background
Foreground τ

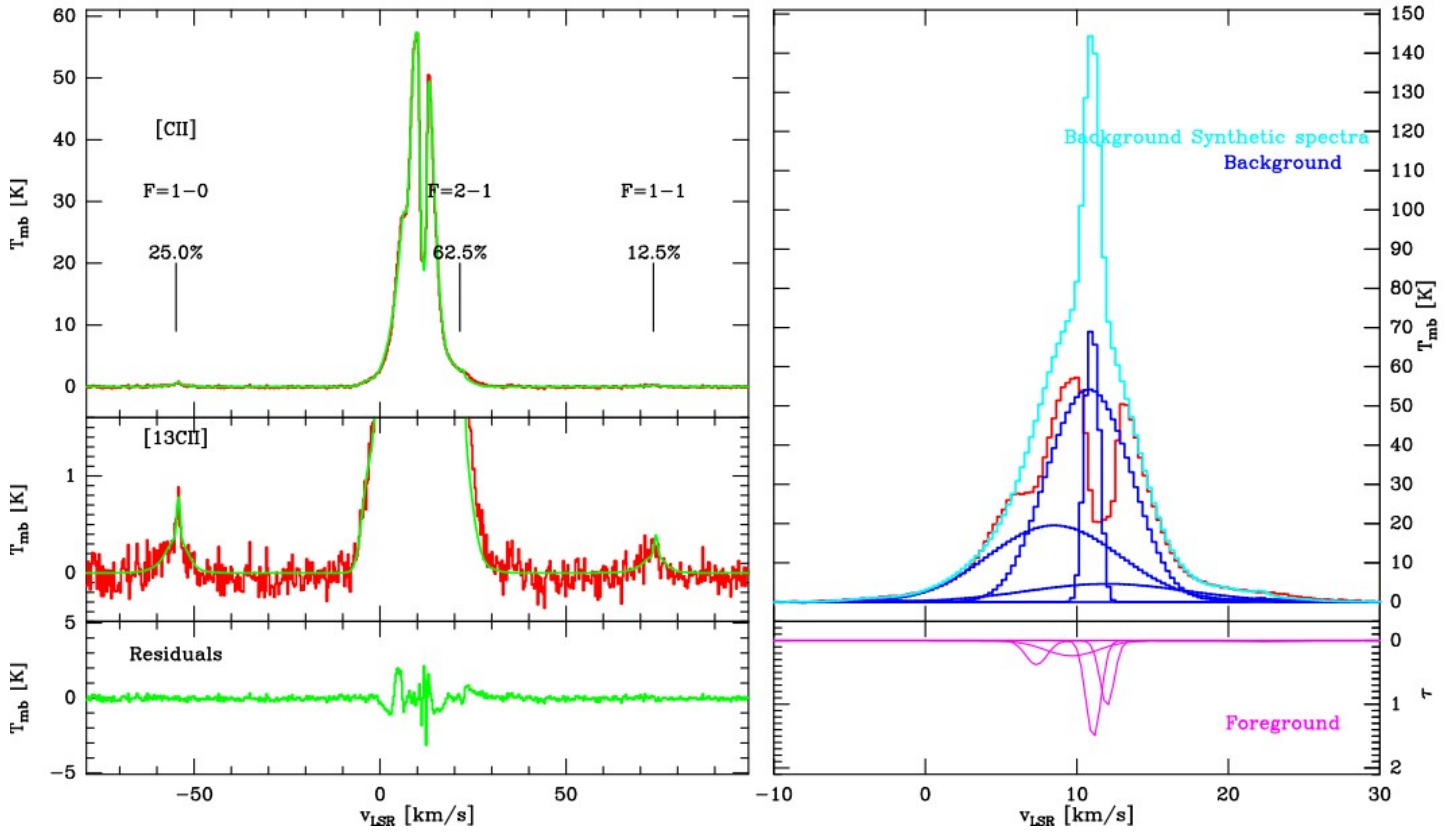

MONR2 position 1

Multi-component Analysis

- **M17SW fitted parameters**

	Background	Foreground
Excitation temperature T_{ex}	180-250 K	20 - 45 K
Column Density (N(CII))	$3x10^{18}$ – $9x10^{18}$ cm^{-2}	$4x10^{17}$ – $3x10^{18}$ cm^{-2}
Equivalent visual extinction (Av)	12 - 41 mag	2 – 13 mag

Model
Data
Background
Foreground τ

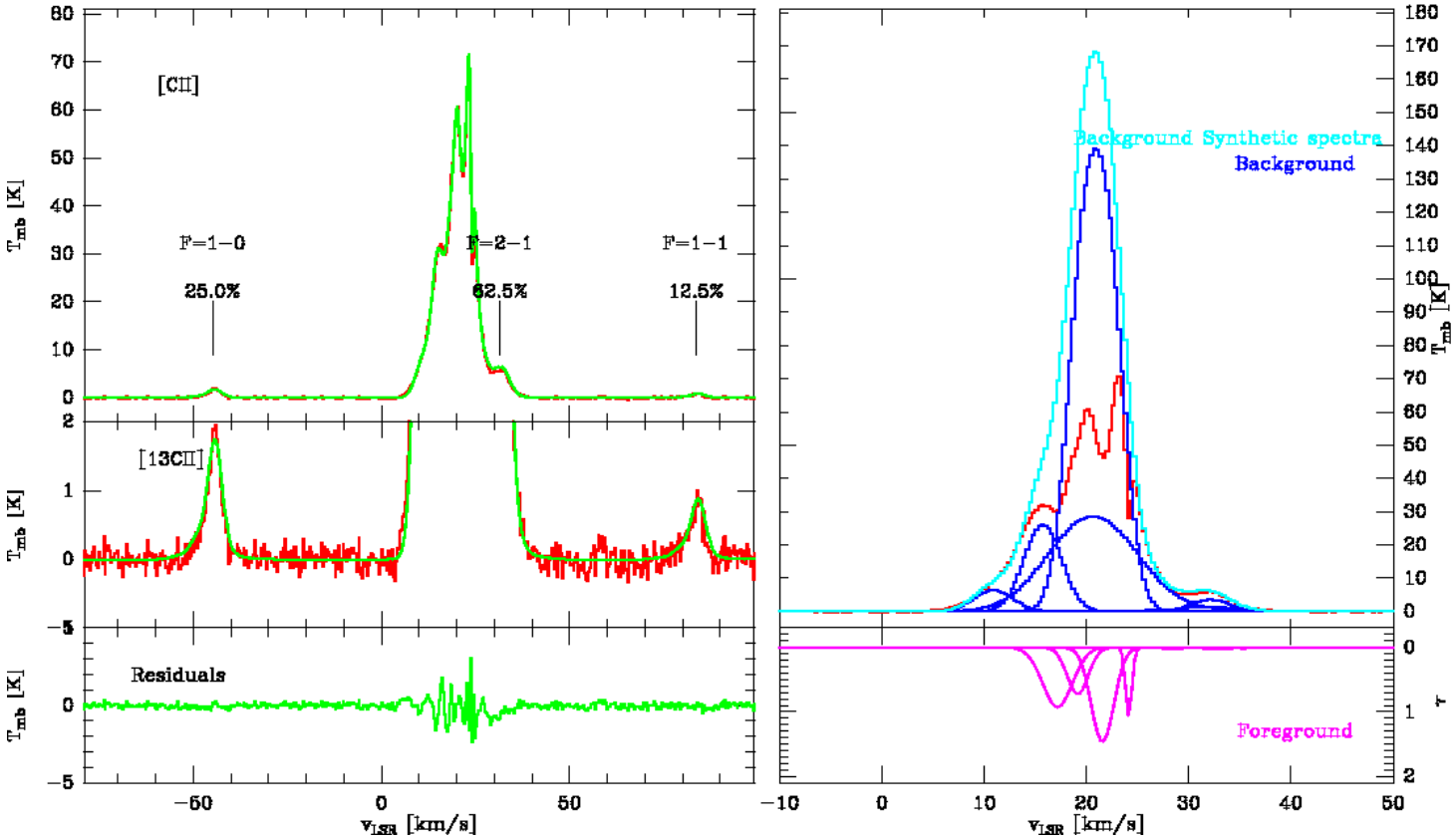

M17SW position 6

Cristian Guevara,
Ph1, Uni zu Köln

Multi-component Analysis

- **An alternative scenario was also studied, a multi-component single emission layered model.**
- **The result shows two kinds of components.**

  - Cold high density gas with a flat-top [^{12}CII] profile due to extremely high optical depth that contributes to the [^{13}CII].

  - Warmer, lower density gas with narrow [^{12}CII] profiles tracing the velocity peaks of the [^{12}CII] emission with negectable emission in [^{13}CII].
- **This scenario was discarded as physically improbably.**

M17SW position 6
Single layer model

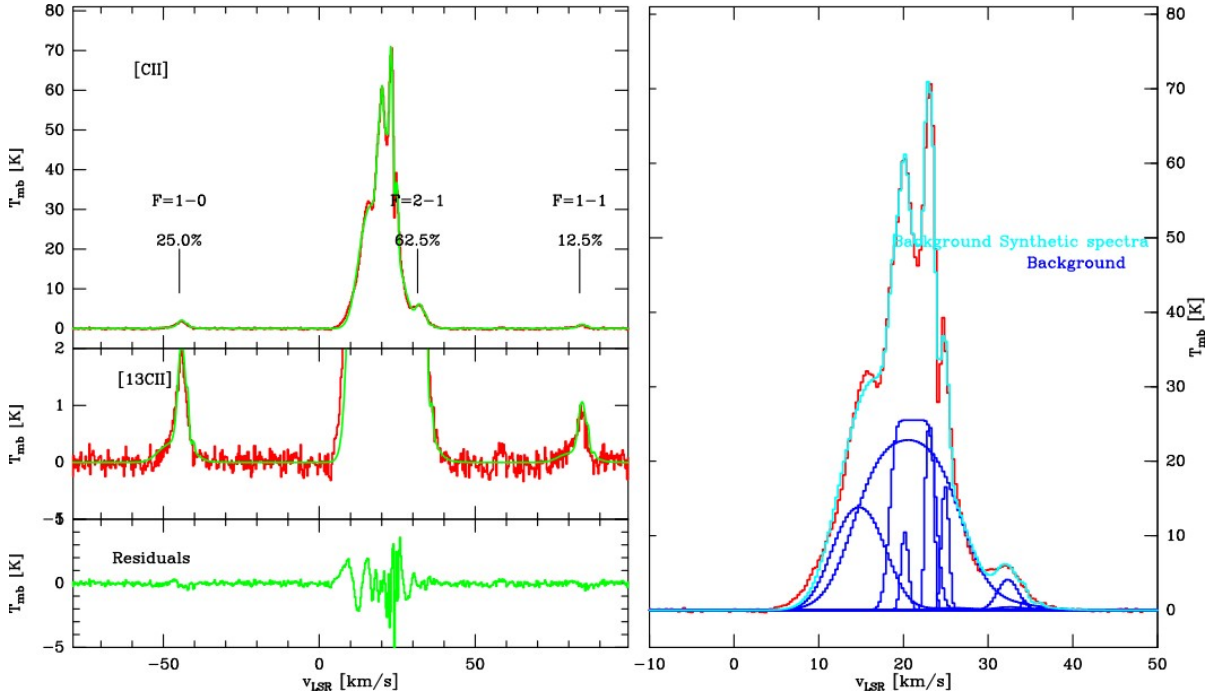

Cristian Guevara,
Ph1, Uni zu Köln

[^{12}CII]/[^{13}CII] Abundance Ratio

- **The analysis highly depends on the assumed ratio, it could be possible to derive the ratio directly from the wing emission with high S/N.**
- **For M17SW, six of the seven positions were averaged to analyze the ratio.**

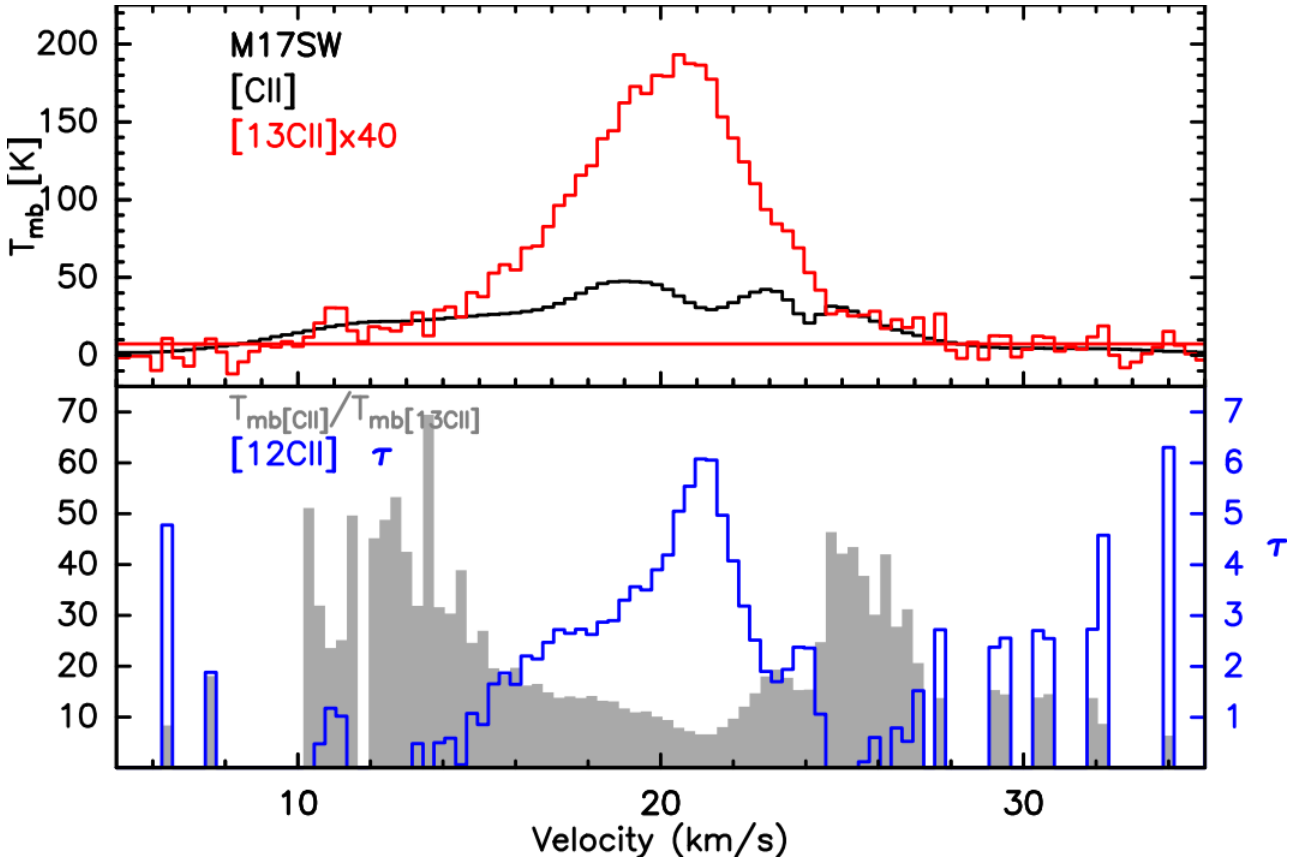

M17SW average spectra

[NII] Observations

- We estimate the [NII] column density under some basic assumptions (T = 8000 K, peak of fractional population in $^3P_1$ and an electron density of 100 cm^{-3})
- The derived column density represents a lower limit.

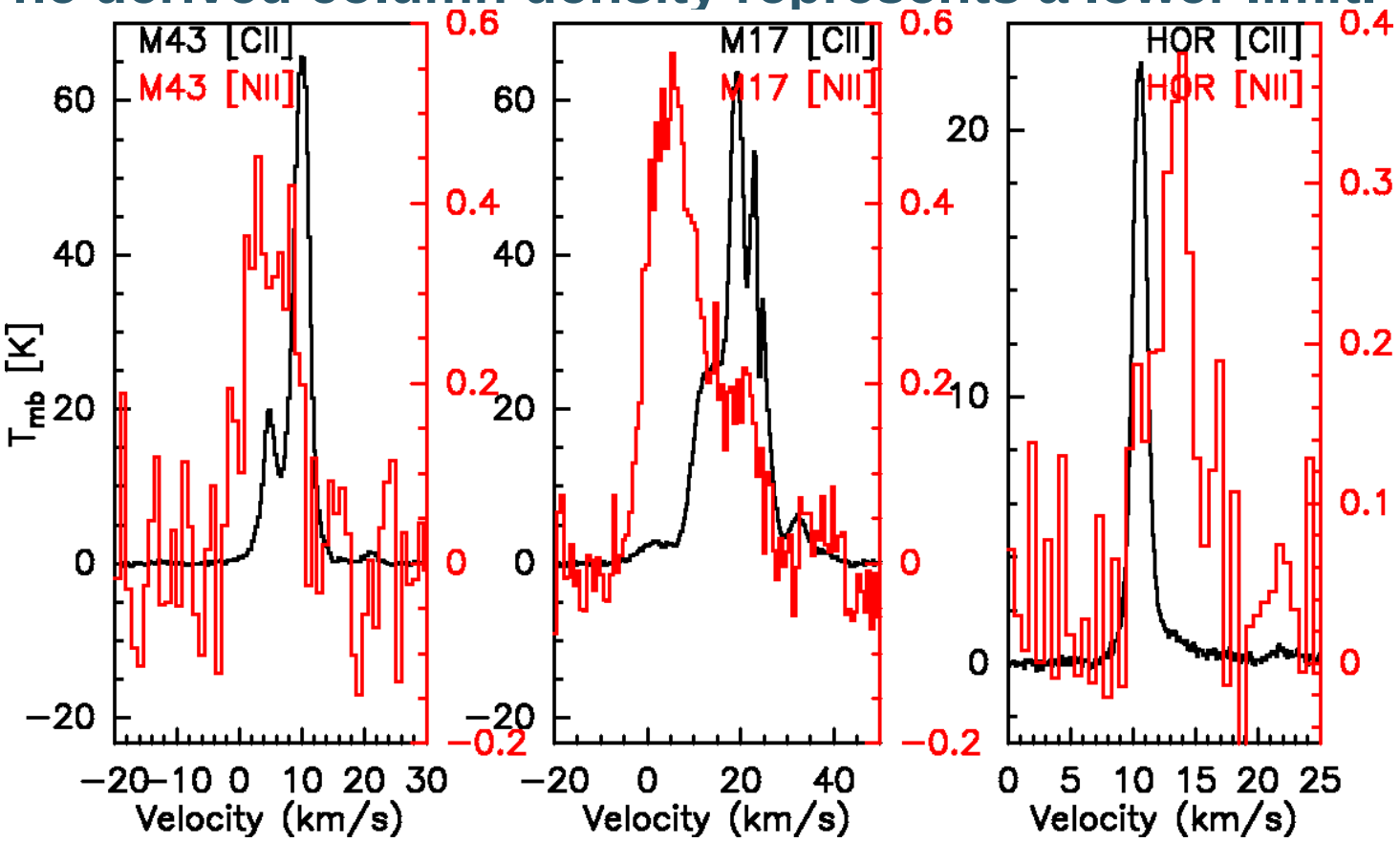

Sources	N(NII) (cm^{-2})	$N(H^+)$ [NII] (cm^{-2})	A_V [NII] (mag.)
M43	1.43E16	2.80E20	0.14
HOR PDR	1.21E16	2.37E20	0.13
M17 SW	3.84E16	7.53E20	0.40

Cristian Guevara,
Ph1, Uni zu Köln

Origin of the Gas

- **High column densities are hard to explain in the standard scenario, high column densities would require several layers of C^+ stacked on top of each other.**
- **For the foreground, it is required low temperature ionized carbon gas, but it is not diffuse gas ($n \sim 10^3\ cm^{-3}$). There are variations in the line profiles between the positions.**

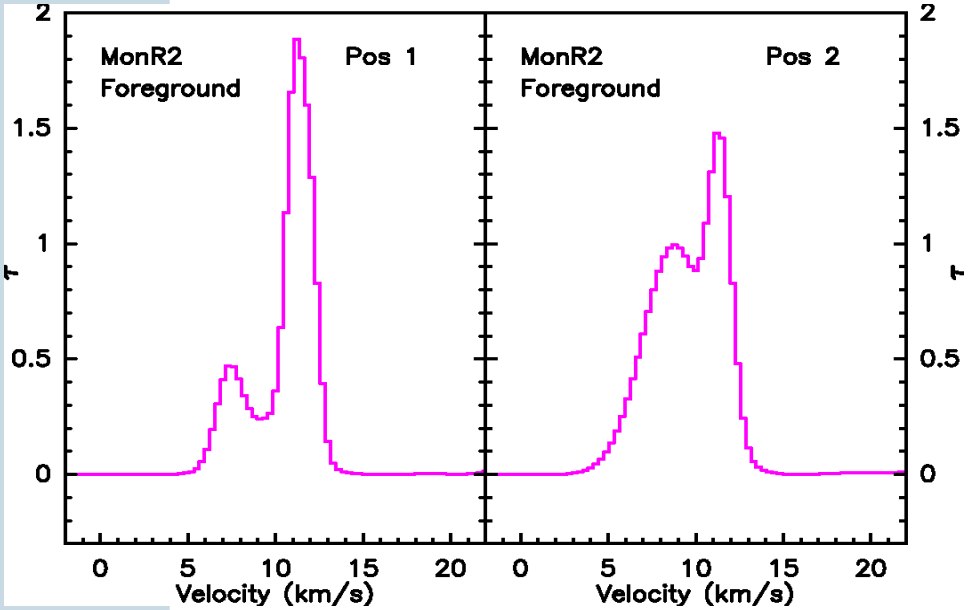

MonR2 foreground line profiles

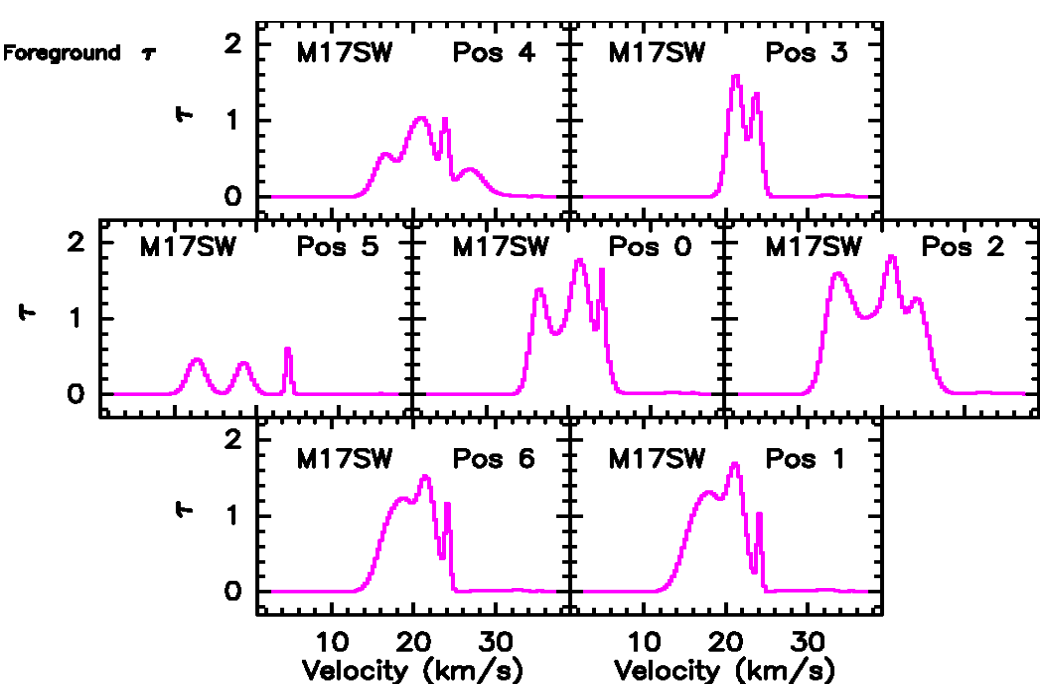

M17SW foreground line profiles

Summary

- **The observations and analysis confirm the long standing suspicion, already proved for the single case of Orion-B (Graf et al 2012). that the [^{12}CII] emission is heavily affected by self-absorption effects and high optical depth.**

- **The absorbing dips change the profile of the [CII] line, mimicking separate velocity components.**

Cristian Guevara,
Ph1, Uni zu Köln

Summary

- **The high column densities of the warmer background are difficult to explain in the present PDR-model context and ISM phases.**
- **The large A_v derived here can be interpreted as several layers of C^+ stacked on top of the other. This situation could be enhanced by fractal and clumply material.**
- **For the foreground, the nature of the material is much more puzzling. The [CII] is ionized, cold lower density material. It is not diffuse gas.**

Future Work

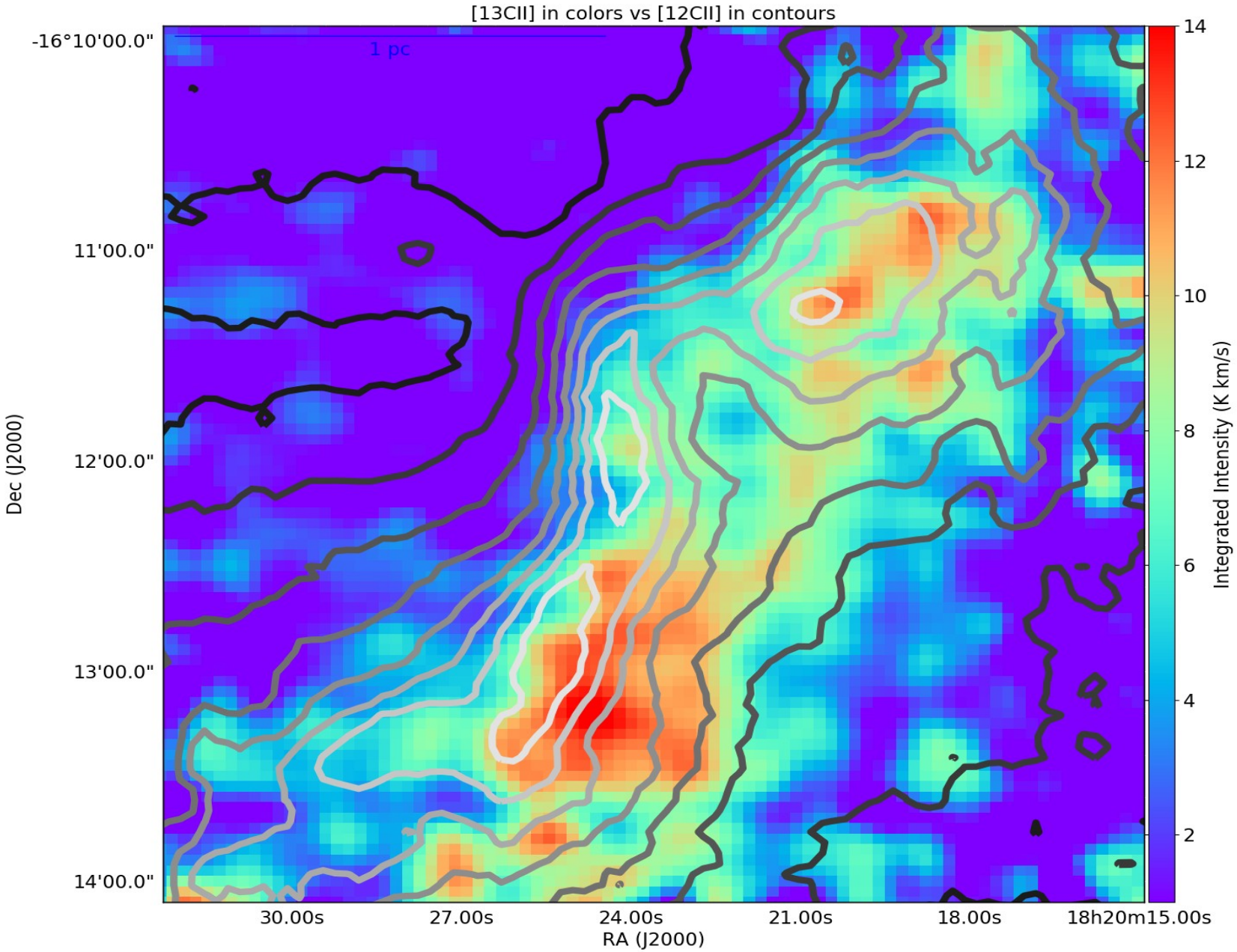

M17SW Integrated intensity map

Cristian Guevara,
Ph1, Uni zu Köln

Future Work

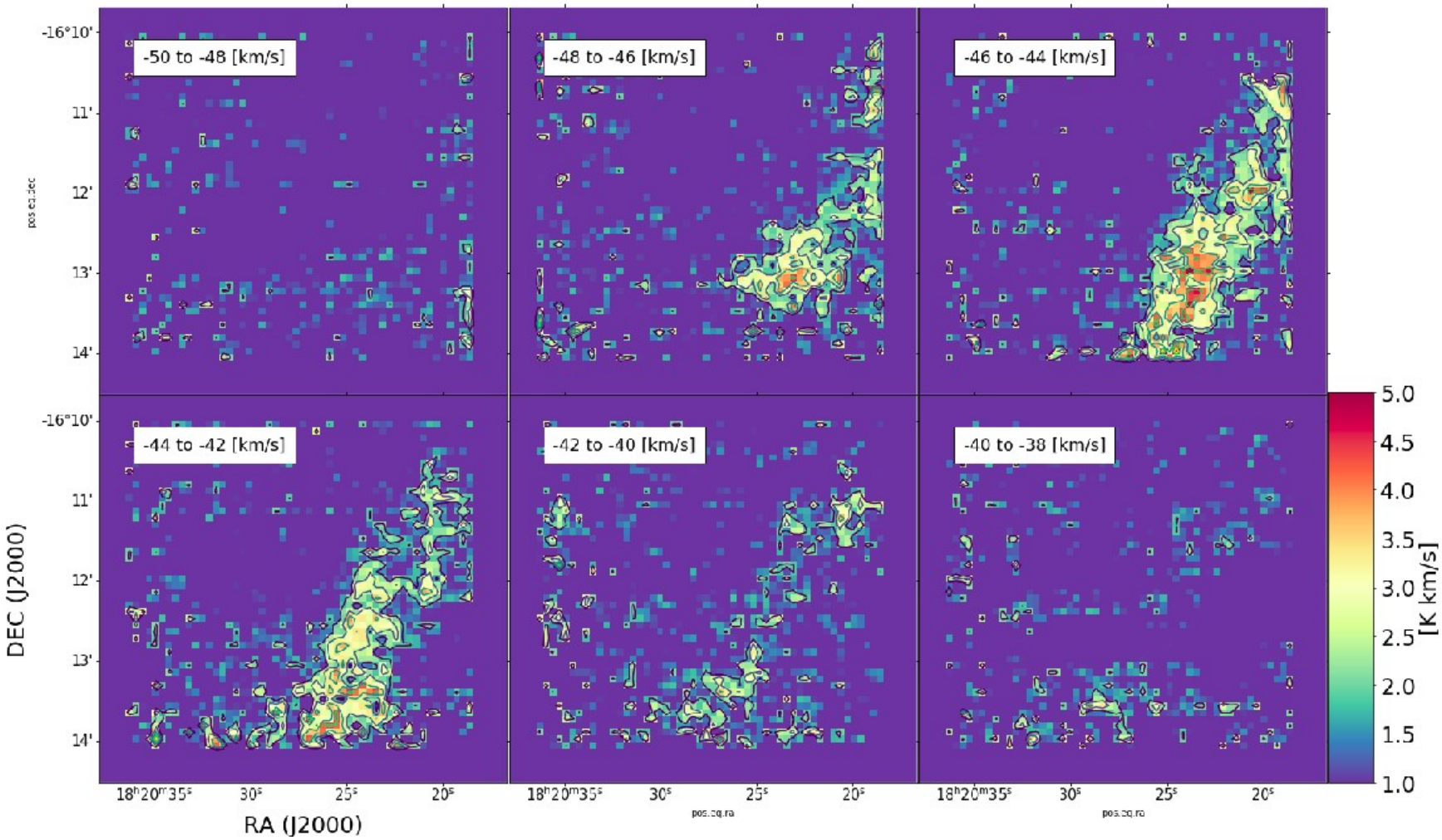

M17SW [^{13}CII] Integrated intensity channel maps

Cristian Guevara, Ph1, Uni zu Köln

Future Work

Feedback Legacy Project

- **Feedback is a SOFIA legacy project using the upGREAT heterodyne receiver to map the [CII] 158 um line in Galactic Molecular clouds.**

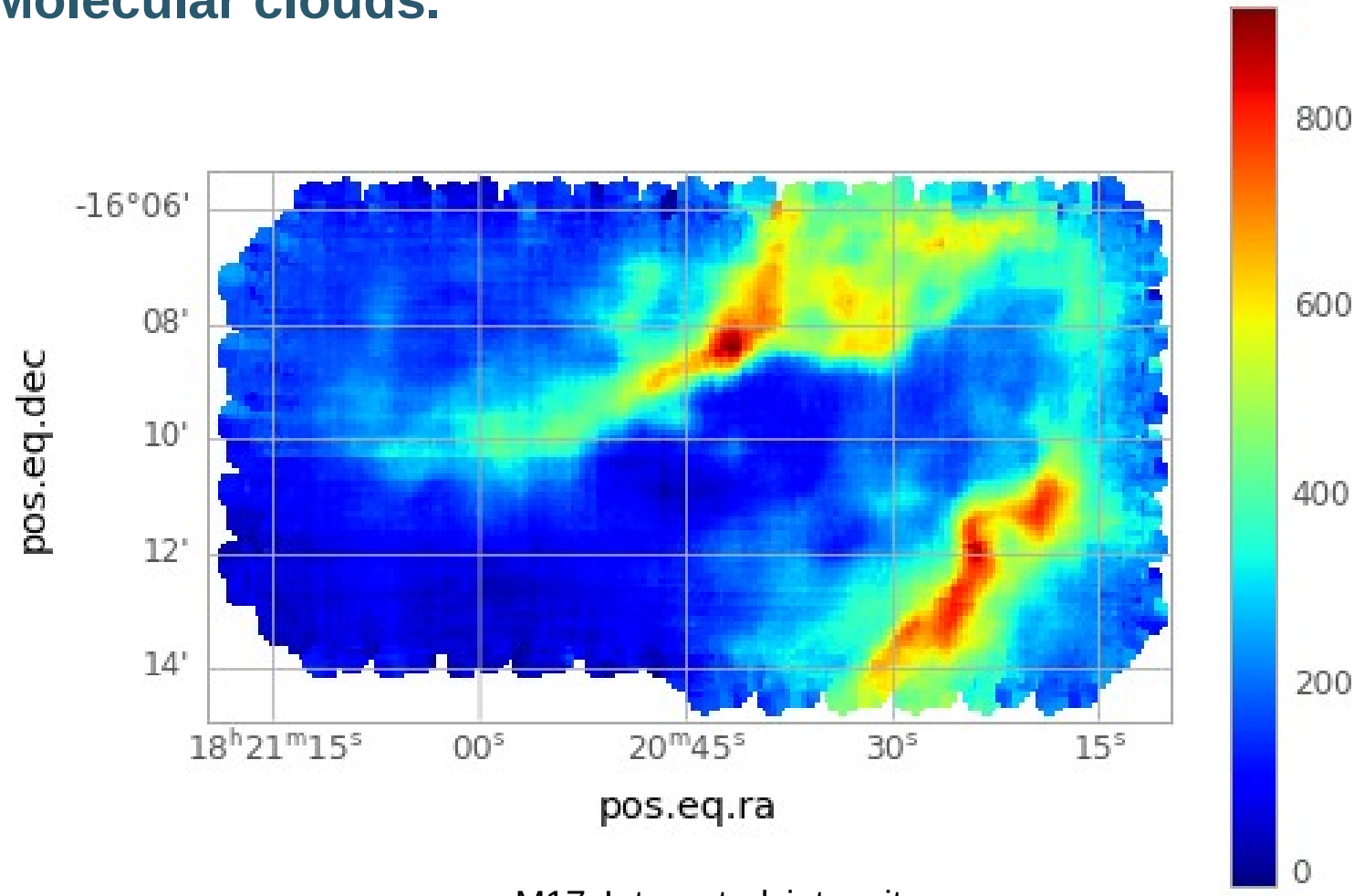

M17 Integrated intensity map observed by FEEDBACK

Future Work

- **Analysis of the average optical depth per regions of RCW120 from the Feedback Legacy Project (Kabanovic et al. in prep)**

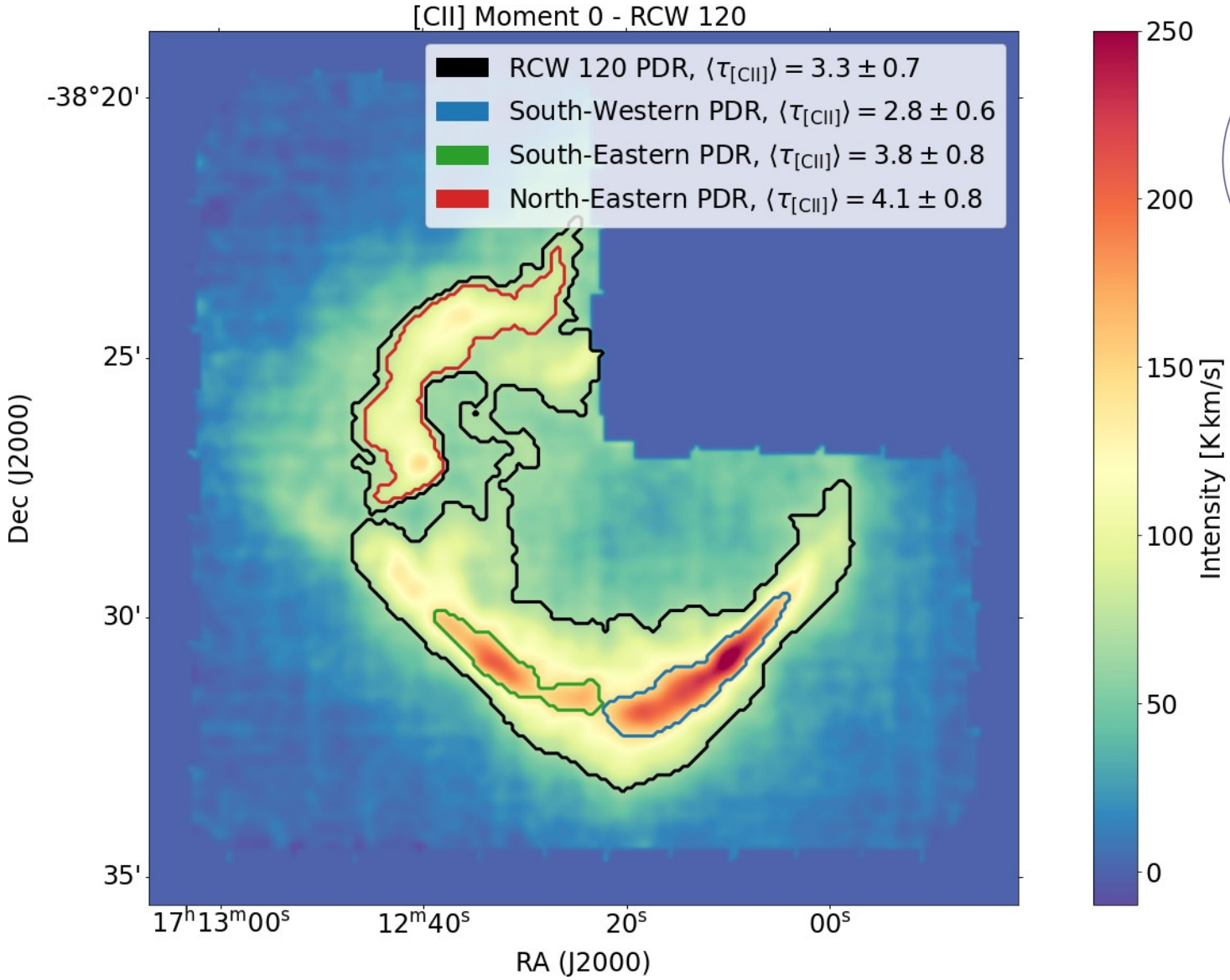

Cristian Guevara,
Ph1, Uni zu Köln

Future Work

- [OI] 63 um also is affected by self-absorption effects, following the same [^{12}CII] absorption dips
- [OI] 145 um seems to be optically thin with a profile similar to the [^{13}CII] emission.

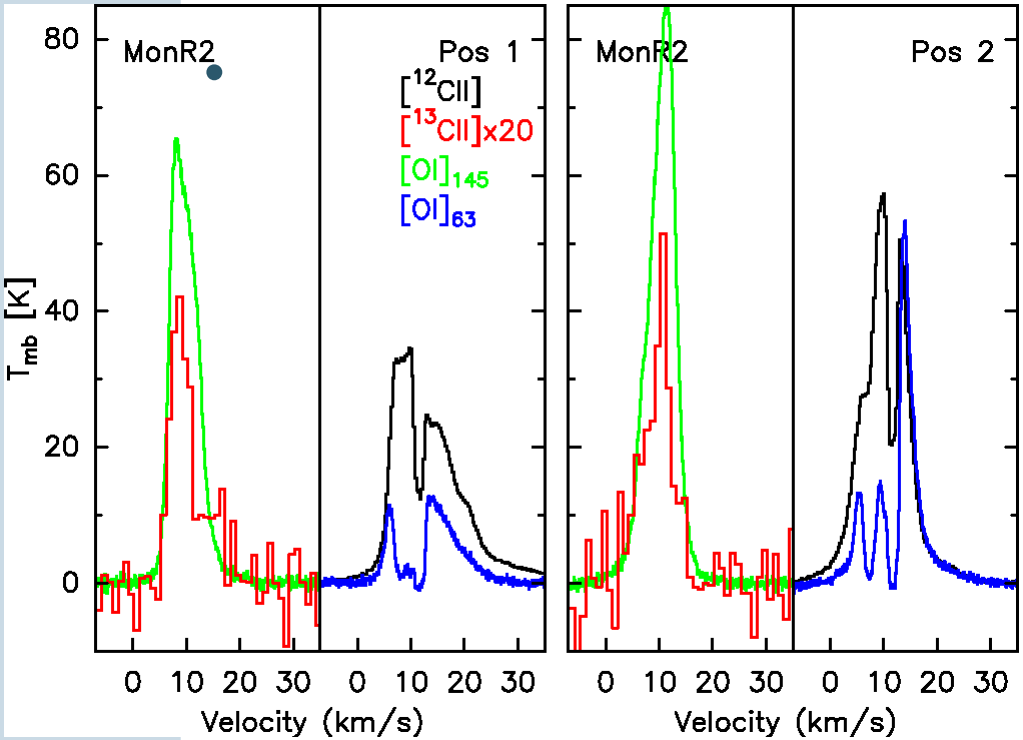

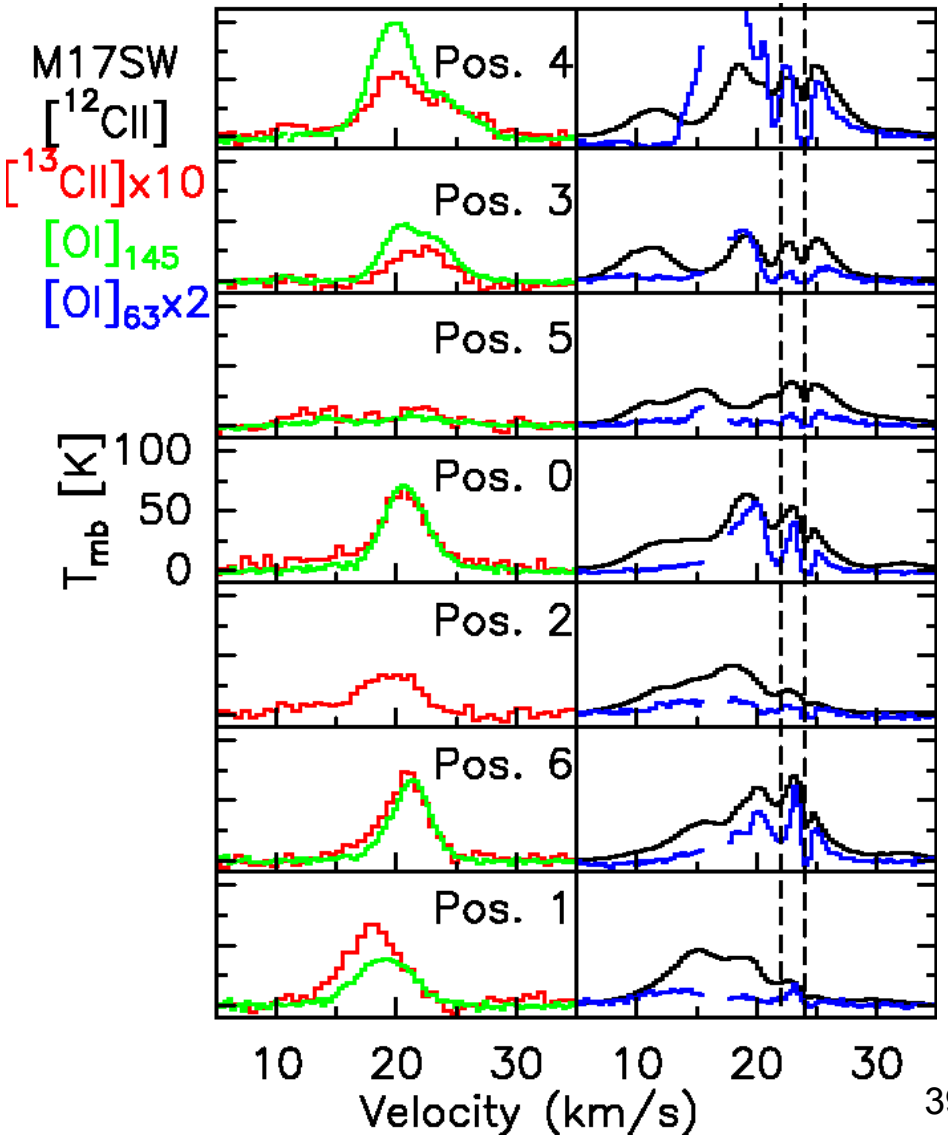

Cristian Guevara,
Ph1, Uni zu Köln

Future Work

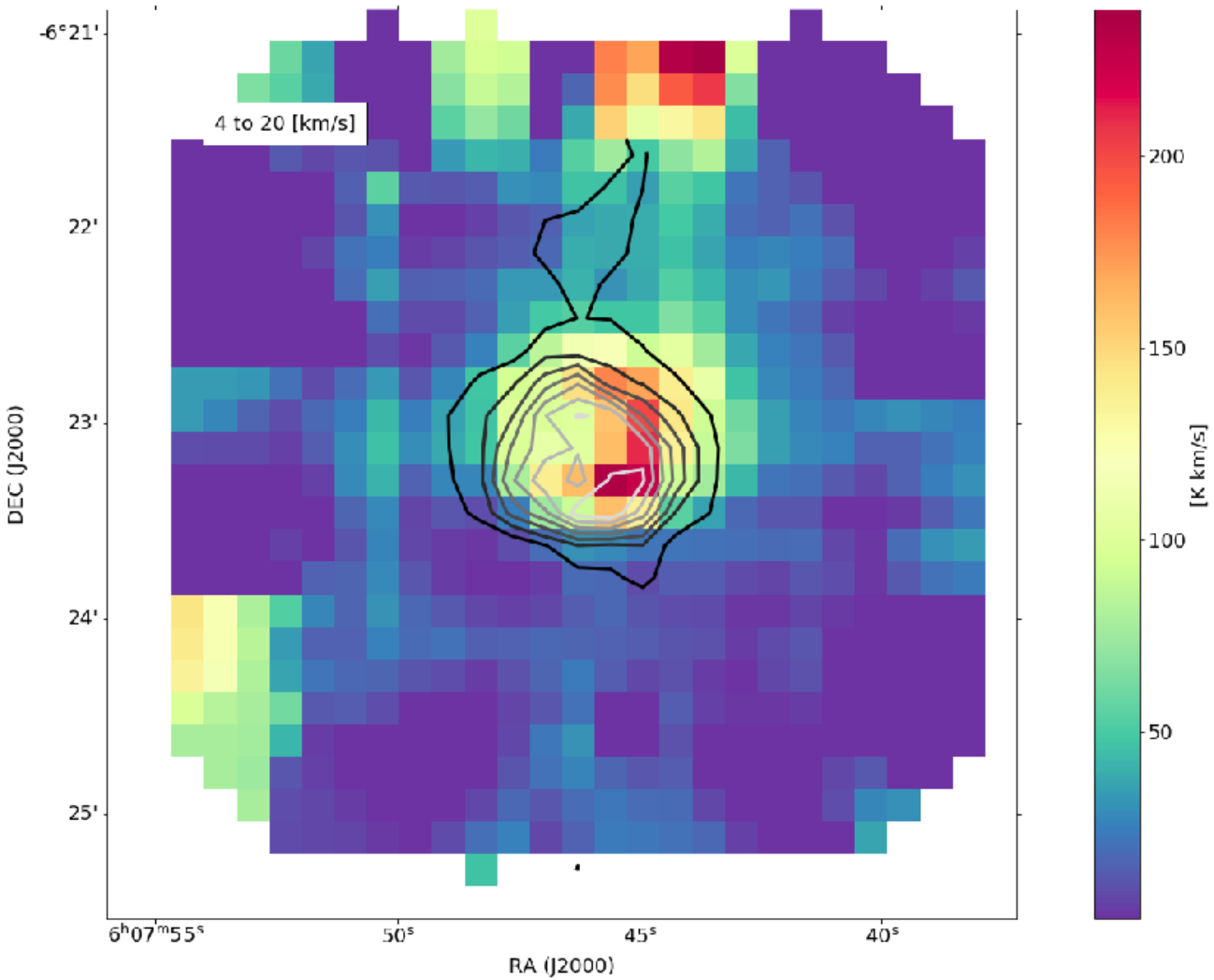

MONR2 [OI] 63 um in colors and [OI] 145 um in contours

Cristian Guevara,
Ph1, Uni zu Köln

Future Work

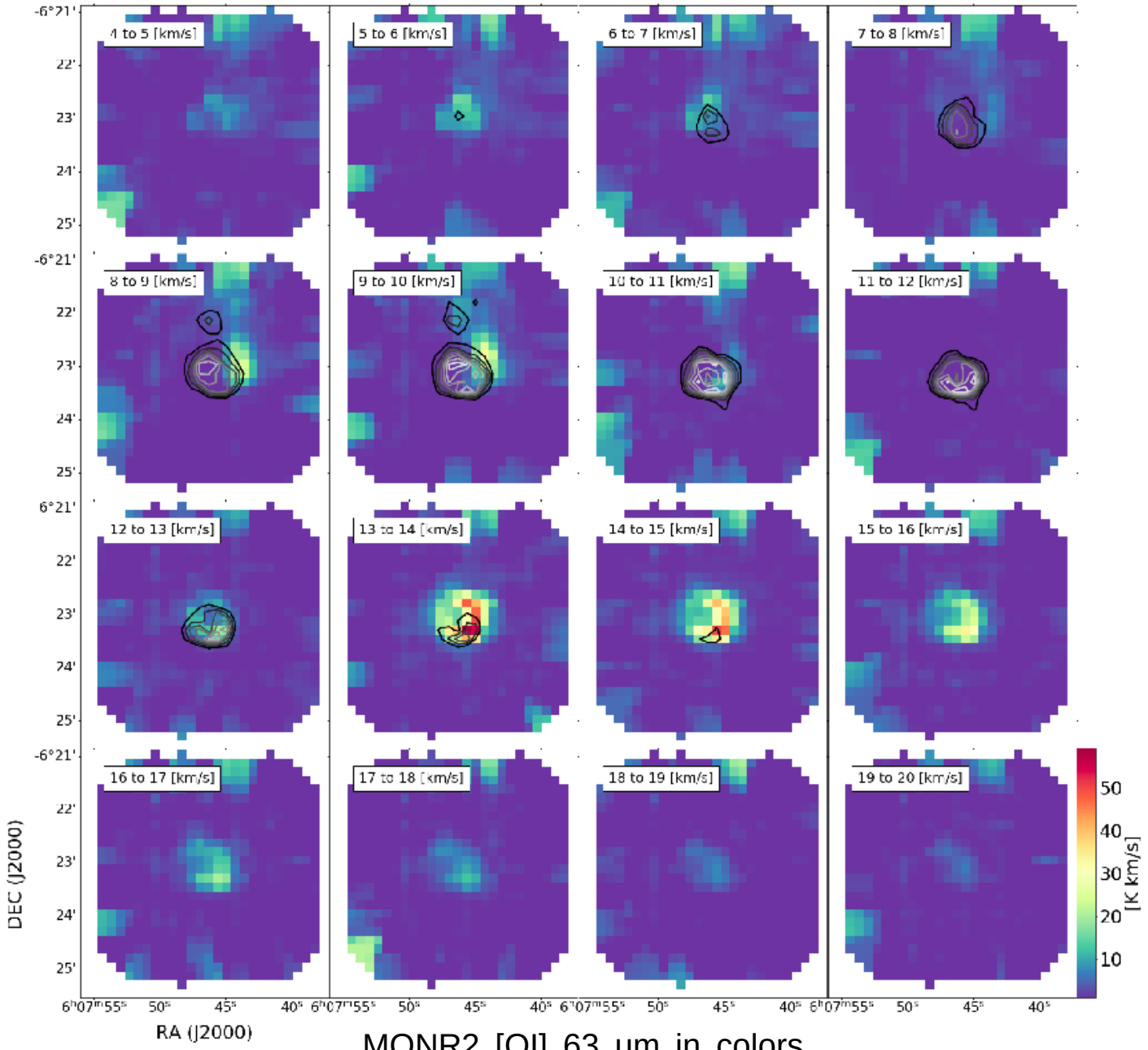

MONR2 [OI] 63 um in colors
and [OI] 145 um in contours

Thank you for your attention

Paper: [C II] 158 μm self-absorption and optical depth effects

https://ui.adsabs.harvard.edu/abs/2020A%26A...636A..16G/abstract